

Addis Ababa  
University

(Since 1950)



**ADDIS ABABA UNIVERSITY**  
**SCHOOL OF GRADUATE STUDIES**  
**DEPARTMENT OF EARTH SCIENCE**

**Analysis and Mapping of Soil Salinity levels in Metehara  
Sugarcane Estate Irrigation Farm using Different Models**

**Thesis Submitted in Partial Fulfillment of the Requirements for the  
Degree of Master of Science in Remote Sensing and  
Geographical Information Systems (GIS)**

**By: Afework Mekeberiaw**

**Advisor: Dr. K.V.Suryabhagavan**

**July, 2009**

**ADDIS ABABA UNIVERSITY**  
**SCHOOL OF GRADUATE STUDIES**  
**DEPARTMENT OF EARTH SCIENCE**

**Analysis and Mapping of Soil Salinity levels in Metehara Sugarcane  
Estate Irrigation Farm using Different Models**

**By Afework Mekeberiaw**

**Thesis Submitted in Partial Fulfillment of the Requirements for the Degree of Master of  
Science in Remote Sensing and Geographical Information Systems (GIS)**

**Approved By Board of Examiners:**

Dr. Balemual Atnafu

Chairman, Department

Graduate Committee

---

Dr. K.V. Suryabhagavan

Advisor

---

Dr. Mekuria Argaw

Examiner

---

Prof. M. Balakrishnan

Examiner

---

## **Acknowledgments**

First and for most, I would like to thank ‘Almighty God’, who made it possible, not only to begin and finish this work successfully, also for his protection and favour in my entire life.

Many thanks to my advisor, Dr. K.V. Suryabhagavan, who patiently read and edited the manuscript and provided me valuable comments and advices throughout my thesis work. I would like to express my gratitude to Dr. Dagnachew Legesse, Remote Sensing and GIS Program Coordinator, for allowing me to develop a sense of independent work personality and for his constant help.

I am also thankful to the officials of Headquarter of Metehara Sugar Factory, particularly to Ato Berhanu Mulu and Ato Abdulazez Yesuf, who provided me various ancillary data. Have no words feeling to my family (Mame, Eshteye and Bezeye) for their financial and material support as well as constant encouragements to mould me as what I am on the present state, without whom my life would not have been successful.

I would like to thank my best friends: Dawite, Gedeyone, Yone and Zembo for providing me different technical materials and advice that was necessary for the completion of this thesis.

I would like to extend my acknowledgement to my brothers Yared and Eskinder for encouraging me throughout my study and Desalegn Lema for helping me in all aspect to finish my research on time.

Last but not the least, I would like to convey my special thanks to my colleagues Alemayehu Degefa , Andualem Aklilu and Nuru Hassen for sharing wisdom and experiences as well as spending good time together during the course of the two years graduate program.

# Table of Contents

<b>ACKNOWLEDGMENTS .....</b>	<b>I</b>
<b>LIST OF TABLES .....</b>	<b>V</b>
<b>LIST OF FIGURES .....</b>	<b>VI</b>
<b>ABBREVIATIONS .....</b>	<b>VII</b>
<b>ABSTRACT .....</b>	<b>VIII</b>
<b>1. INTRODUCTION .....</b>	<b>1</b>
1.1 BACKGROUND.....	1
1.2 STATEMENT OF THE PROBLEM .....	2
1.3 OBJECTIVES .....	3
1.3.1 General Objective .....	3
1.3.2 Specific objectives .....	3
<b>2. LITERATURE REVIEW.....</b>	<b>4</b>
2.1 SOIL SALINITY .....	4
2.2 REMOTE SENSING FOR MAPPING SOIL SALINITY.....	5
2.2.1 Salt-affected Soils and Spectral properties .....	6
2.2.1.1 Application at field level .....	6
2.2.2 Water logging.....	8
2.2.3 Application to large areas .....	8
2.2.3.1 Visual interpretation using photo imagery.....	9
2.2.3.2 Digital analysis.....	10
2.2.3.3 Digital analysis using surface vegetation index .....	11
2.3 GIS IN SOIL SALINITY MODELING .....	12
2.3.1 Soil Salinity modeling using multi-criteria decision evaluation.....	12
<b>3. METHODOLOGY .....</b>	<b>14</b>
3.1 DESCRIPTION OF THE STUDY AREA.....	14
3.1.1 Climate.....	15
3.1.2 Geomorphology, Soil and Parent Material .....	16
3.2 METHODS .....	17
3.2.1 Salinity Indices.....	17
3.2.2 Vegetation Indicator.....	17
3.2.3 Empirical Models of Soil Salinity and Spectral Reflectance.....	18

3.2.4 Overlay Soil Salinization Model.....	19
3.2.5 Overlay Analysis.....	20
3.2.6 Spatial Data analysis .....	21
3.2.6.1 Data collection.....	21
3.2.7 Classification of salt affected areas using satellite image analysis.....	21
3.2.7.1 Band Selection.....	21
3.2.7.2 Analyses of the Correlation Matrix.....	22
3.2.7.3 Spectral Classes of Saline Soils .....	22
3.2.8 True and False Colour Composite Image Preparation.....	23
3.2.9 Spatial Distribution of ECe.....	25
3.3 OVERLAY SOIL SALINITY MODEL ANALYSIS.....	29
3.3.1 Salinity Modeling.....	29
3.3.2 Model Parameters .....	29
3.3.3 Multi-Criteria Decision Making .....	40
3.4 OVERLAY ANALYSIS OF SALT AFFECTED SOIL AGAINST DIFFERENT FACTORS .....	41
3.4.1 Preparation features for overlaying.....	41
3.4.1.1 Drainage and Canal Layout.....	41
3.4.1.2 Piezometric data .....	43
3.4.1.3 Soil Map.....	45
<b>4. RESULTS AND DISCUSSION.....</b>	<b>46</b>
4.1 DISTRIBUTION OF THE SALT-AFFECTED AREAS IN THE SUGARCANE FARM .....	46
4.1.1 Salt-affected Areas Characterized by Salinity Levels .....	46
4.1.1.1 Severe saline.....	46
4.1.1.2 Moderate saline .....	46
4.1.1.3 Slight saline .....	46
4.2 RESULT FROM SATELLITE IMAGE CLASSIFICATION .....	47
4.2.1 Results from Supervised Classification .....	47
4.2.2 Results from Indice Analysis .....	49
4.3 EMPIRICAL MODELS USING SOIL SALINITY (EC).....	51
4.4 RESULT FROM OVERLAY SOIL SALINITY MODEL.....	53
4.4.1 Salinity Model.....	53
4.5 VALIDATION AND COMPARISON OF THE METHODS.....	55
4.6 RESULTS FROM OVERLAY ANALYSIS OF SALT-AFFECTED SOIL AGAINST THE DIFFERENT FACTORS.....	56
4.6.1 Canal vs Map of salt affected soil generated from Overlay soil salinity model .....	56
4.6.2 Drainage vs Map of salt affected soil generated from Overlay salinity model .....	57
4.6.3 Soil vs Map of salt affected soil generated from Overlay salinity model.....	58
4.6.4 Water Table vs Map of salt affected soil generated from Overlay salinity model .....	59
<b>5. CONCLUSIONS AND RECOMMENDATIONS .....</b>	<b>61</b>

5.1 CONCLUSIONS.....	61
5.2 RECOMMENDATION .....	62
<b>REFERENCES.....</b>	<b>64</b>
<b>APPENDIX-I .....</b>	<b>68</b>
<b>APPENDIX-II.....</b>	<b>72</b>
<b>APPENDIX-III .....</b>	<b>73</b>

## List of Tables

Table 2.1. The criteria for soil salinity and sodicity.....	4
Table 3.2. Correlation matrix of bands. ....	22
Table 3.3. EC, pH and water table for Metehara Sugarcane Estate. ....	25
Table 3.4. Pair-wise Comparison Matrix .....	40
Table 3.5. Factor weights derived by calculating the Principal Eigenvector of the Pair-wise Comparison Matrix .....	41
Table 3.6. Classification of water depth.....	44
Table 4.1. Salinity level determined from NDSI in percent.....	50
Table 4.2. Salinity level and extent derived from empirical model. ....	52
Table 4.3. Extent of areas of various salinity levels derived from overly salinity model.....	53

## List of Figures

Figure 3.1 Location map of the study area .....	14
Figure 3.2. Classification of salt affected areas by satellite imagery. ....	18
Figure 3.3. Classification of the salt affected areas based on geology, land form, ground water level and land cover. ....	19
Figure 3.4. Overlay analysis of salinity map against soil map, canal layout, drainage layout and ground water level. ....	20
Figure 3.5. Spectral signatures of Metehara sugarcane Estate during May 2005.....	23
Figure 3.6. Different Landsat ETM+ band combinations.....	24
Figure 3.7. EC sample Locations.....	26
Figure 3.8. Regression Analyses between ECe and NDSI. ....	27
Figure 3.9. The model used for prediction of soil salinity.....	28
Figure 3.10. Digital elevation model of Metehara Sugarcane estate. ....	30
Figure 3.11. Land form of Metehara Sugarcane estate.....	31
Figure 3.12. Reclassified Land form of Metehara Sugarcane estate. ....	32
Figure 3.13. Land-cover of Metehara Sugarcane estate. ....	33
Figure 3.14. Reclassified Land-cover of Metehara Sugarcane estate.....	34
Figure 3.15. Geology of Metehara Sugarcane estate. ....	35
Figure 3.16. Reclassified geology of Metehara Sugarcane estate. ....	36
Figure 3.17. Location of Piezometric data. ....	37
Figure 3.18. Interpolated ground water level of Metehara Sugarcane estate. ....	38
Figure 3.19. Reclassified Interpolated ground water level of Metehara Sugarcane estate.....	39
Figure 3.20. Buffered drainage layout of Metehara sugarcane estate. ....	42
Figure 3.21. Buffered Canal layout of Metehara sugarcane estate.....	43
Figure 3.22. Interpolated ground water level classes. ....	44
Figure 3.23. Soil map of Metehara Sugarcane estate. ....	45
Figure 4.1. Land-use land-cover map.....	48
Figure 4.2. Aerial extent of soil salinity derived from land-use land-cover map.....	48
Figure 4.3. Map of Normalized Difference Salinity Index (NDSI).....	50
Figure 4.4. Salinity map generated from empirical model. ....	52
Figure 4.5. Salinity level derived from overlay salinity model. ....	54
Figure 4.6. Salinity map of Metehara sugarcane estate generated from overlay salinity model.....	54
Figure 4.7. Correlation of ECe and raster value of NDSI. ....	55
Figure 4.8. Correlation of ECe and raster value of overlay salinity model. ....	56
Figure 4.9. Salt affected area vs canal. ....	57
Figure 4.10. Salt affected area vs surface drainage lines.....	58
Figure 4.11. Salt affected areas vs major soil types of the study area. ....	59
Figure 4.12. Spatial Distribution of salt affected soil vs water table depth.....	60
Figure 4.13. Salt affected areas vs water table depth. ....	60

## Abbreviations

<b>DEM</b>	Digital Elevation Model
<b>dS/m</b>	Decisiemens per meter
<b>ECe</b>	Electrical conductivity of the saturation extract of soil
<b>ESP</b>	Exchangeable Sodium Percentage
<b>ETM+</b>	Enhanced Thematic Mapper plus
<b>FCC</b>	False Colour Composition
<b>GIRDC</b>	Generation Integrated Rural Development Consultant
<b>GIS</b>	Geographic Information System
<b>IAR</b>	Institute of Agricultural Research
<b>IRS</b>	Indian Remote Sensing
<b>LAI</b>	Leaf Area Index
<b>MSF</b>	Metehara Sugar Factory
<b>MSS</b>	Multi-Spectral Scanner
<b>NDSI</b>	Normalized Difference Salinity Index
<b>NDVI</b>	Normalized Difference Vegetation Index
<b>NIR</b>	Near Infrared
<b>pH</b>	Power of Hydrogen
<b>RGB</b>	Red, Green, Blue
<b>SRTM</b>	Shuttle Radar Topography Mission
<b>TDS</b>	Total Dissolved Solid
<b>TIR</b>	Thermal Infrared
<b>TM</b>	Thematic Mapper
<b>TCC</b>	True Colour Composite
<b>USDA</b>	United State Department of Agriculture

## Abstract

This thesis deals with the analysis and mapping of soil salinity levels in Metehara sugarcane estate irrigation farm. An attempt was made to identify salt affected areas by visual interpretation using both true and false colour composite. From the supervised classification, 726 ha area was mapped as highly saline. However, the result obtained from NDSI was not only in area-wise, but also the level of salinity as highly saline, moderately and slightly saline, determined based on the reflectance value. Out of the total area, 6% was mapped as highly saline. A regression analysis between EC values of small areas confined only in Metehara Sugarcane estate and the corresponding reflectance value in the NDSI image offer a polynomial relation of order two. The empirical model that obtained from the regression analysis was used to derive a salinity map and estimate EC level. The spatial distribution of salt affected area derived from NDSI and model were of similar pattern but of different extent. In overlay salinity model, four classes have been identified with varying degree of salinity. The class of highly saline soils was found in the areas underlain by the lacustrine Sediments and shallow ground water level. It is evident that the areas highly vulnerable to salinization greatly related to the ground water level that normally occurred on the lacustrine sediment near to lake Beseka. The validation of the two models has been carried out by the existing EC values referenced to the same locations by making linear correlation. The correlation shows that overlay salinity model to be a better indicator of soil salinity than empirical model in the study area. Since empirical model detects only the salts on the surface of the soil and gives a poor idea about the conditions below surface, the overlay salinity model indicates the condition and existence of salt in the entire soil section between the surface and root zone. Then overlay analysis between salt affected areas and canal, drainage, water table and soil was made to assess the spatial distribution as well as the relationship with these features. It was revealed that the spatial distribution was not highly influenced by the features considered except water table.

*Key words: EC, NDSI, Soil salinity, Empirical Model, Overlay Salinity Model*

# **1. Introduction**

## **1.1 Background**

Soil salinity and/or sodicity is a major land degradation problem in many part of the world. The development of salt affected soils and associated problems are most pronounced in arid and semi arid regions, which offer considerable promise for development as major food producing regions, because of their frequent potential for multiple cropping. Irrigation, evaporation of moisture from the surface or shallow depths within the profile, and the insufficient annual rainfall to leach down salts from the plant rooting zone favour excessive accumulation of soluble salts in soils of arid and semi arid regions, rendering such lands to have been used by human beings with only marginal success since the advent of agriculture. As a result, the study of arid lands and salt affected soils has been important throughout the history of agricultural development (Dwivedi, 1996).

Partial or complete loss of soil productivity attributed to accumulation of excess salts in the root zone of soils in the arid and semi arid climates is a worldwide phenomenon. However, the most serious salinity and sodicity problems are being faced in the irrigated arid and semi arid regions of the world and it is in these regions that irrigation is essential to increase agricultural production to satisfy food requirements. Soil salinity is also a serious problem in areas where groundwater of high salt content is used for irrigation. On the other hand, irrigation is often costly, technically complex and requires skilled management. Failure to apply efficient principles of water management may result in wastage of water through seepage; overwatering and inadequate drainage resulting in water logging and salinity/sodicity problems, which reduce the soil productivity, eventually leading to loss of cultivable land. Thus, development of technology to control and mitigate salinity and sodicity is particularly an important issue for modern agricultural management, especially for countries such as Ethiopia where arid and semi arid climatic zones occupy over 60% of the total land area (OWWDSA, 2007).

Generally, the main sources of salinity are shallow ground water tables, natural saline seeps irrigation waters, source from marine origin and fertilization. The world's total land area under

salt affected soils at the present time is estimated at over 950 million ha, approximately. Approximately 40 or 50% of the irrigated land in the arid and semi arid regions in the world has some degree of soil salinity and/or sodicity problems. Moreover, an estimated land area of 405 million ha in the world is with saline aquifers. As a result, over 6 million ha of the land of our planet is estimated to be lost each year to salinity, sodicity and drainage problems (Szabolcs, 1987).

## **1.2 Statement of the Problem**

In Ethiopia, approximately 11 million ha land is salt affected (Fantahun Abegaz, 2007). These areas are mainly concentrated in the Rift Valley, Wabi Shebelle River Basin and various other lowlands and valley bottoms. For instance, it has been reported that of the 4,000 hectares of irrigated lands at Melka Sedi, about 40.0, 16.98 and 0.02% were saline, saline sodic and sodic, respectively. Similar reports also indicate that a considerable extent of area of land has been abandoned for cultivation due to the prevalence of salt affected soils at the Middle Awash. Furthermore, recent reports also indicate that 39% of the Abaya State Farm is salt affected. These figures indicate the magnitude of the problem that must be tackled in order to meet future national food needs of the increasing population, which is generally agreed to be met by directing the efforts of all concerned towards improving the level of management of soils already under cultivation, and by bringing new areas, in practice new areas of the dry land ecosystems, under cultivation (OWWDSA, 2007).

The problems of salt affected soils are old, but their magnitude and intensity have been increasing fast due to the establishment of large-scale irrigated farms in recent decades. Inadequate provision of drainage system and poor water management practices coupled with unsound reclamation procedures have made the problem worse. In general, 2,280 ha (Melka Sedi), 500 ha (Metehara), 300 ha (Asayta), 220 ha (Kebena or Yalo), 145 ha (Kesem), 100 ha (Gewanie), 56 ha (Werer State Farm), 80 ha (Shoa, Kefa Dura), 20 ha (Millie) and some areas at Tangay Kuma State Farm have proved to be salt affected. Moreover, it is expected that the salt affected soils in these areas will dramatically increase in the coming few years if the current irrigation practice is allowed to continue (Fantahun Abegaz, 2007).

Mapping of the land damaged due to salinization is a frantic task and requires lot of man-power and time since it requires identification, sampling and classifying the land by conventional surveying methods. On the other hand, advanced techniques like Remote Sensing (RS) and Geographical Information System (GIS) can do this task more efficiently. The approach to the problem dealing with salt affected land using RS and GIS has been proved in many recent studies to be the most efficient (Rao *et al.*, 1997). Large coverage, good resolution in visible and near visible spectrum and repetitive passes are advantages of RS satellites and advanced analytical techniques in GIS can be useful in detection and intensity analysis of salt affected land (Moulders, 1987).

## **1.3 Objectives**

### **1.3.1 General Objective**

- ❖ The general objective of this study is to assess salinity and sodicity problems in different parts of a large scale mechanized irrigation farm in the Metehara sugarcane area of the middle Awash to map the distribution of the problem over the whole area, which might be useful for effective management of salinity problem and thereby prevention of it in the future.

### **1.3.2 Specific objectives**

- ❖ To identify and map salt affected soils by empirical and overlay methods.
- ❖ To apply different salt indices to detect salt affected area.
- ❖ To identify the best method for salt affected soil mapping.
- ❖ To assess and evaluate the spatial distribution of salt affected soils against irrigation canal, drainages, soil types and water tables.

## 2. Literature Review

### 2.1 Soil Salinity

Several agencies have given different definitions for soil salinity. The most widely accepted definition of salt-affected soils is as defined by the United States Department of Agriculture, (USDA) (Richards, 1954). The definition is based on ECe (electrical conductivity of the saturation extract of soil,  $\text{dSm}^{-1}$ ), pHs (pH of the saturated soil paste) and ESP (exchangeable sodium percentage of the soil).

**I. Saline soils:** These soils have an ECe more than  $4 \text{ dSm}^{-1}$  at  $25^{\circ}\text{C}$ , pHs less than 8.2, and ESP less than 15.

**II. Sodic soils:** Sodic soils have a pHs more than 8.2, and ESP of 15 or more. The ECe may be high if originating from salts capable of alkali hydrolysis; otherwise it should be less than  $4 \text{ dSm}^{-1}$  at  $25^{\circ}\text{C}$ .

**III. Saline-Sodic:** Saline-sodic soils have pHs greater than 8.2 at  $25^{\circ}\text{C}$ , ECe greater than  $4 \text{ dSm}^{-1}$  and the ESP greater than 15. These soils have formed due to a combined process of salinization and sodification.

A general guideline for the degree of soil salinity/sodicity is given in Table 2.1; however, the severity may vary with the type of soil and crop.

Table 2.1. The criteria for soil salinity and sodicity.

Key to degree of salinity/sodicity	Salinity ECe( $\text{dSm}^{-1}$ )	Sodicity	
		pH	ESP
Slight	4-8	8.2-9.0	<15
Moderate	8-25	9.0-9.8	15-40
Strong	>25	>9.8	>40

## **2.2 Remote sensing for mapping soil salinity**

The essence of remote sensing is the measuring and recording of the electromagnetic radiation emitted or reflected by the earth's surface. For soil salinity investigation, this may be useful where salty soil, salt-affected vegetation, saline water, pond water and high water table area give contrasting reflectance with other landscape features so that they can be unambiguously distinguished.

Application of remote sensing for surveying and mapping of salt-affected areas began with the use of black and white photography. The relatively bright appearance provides the information about salinity due to the efflorescence of salt crust. The effect of salinity on crops provides the information on salinity indirectly. The aerial photographs have been used to delineate units based on the combination of geomorphological differences and differences in grey tones. Attempts were also made to relate the differences in the grey tones with the salt content. After the launch of the first operational earth observation satellite, Landsat in 1972, with visible and near infrared bands, it became easy to map large areas and to repeat mapping frequently. For the appraisal of soil salinity problems, spectral, spatial and temporal characteristics of these twin problems are to be considered to assess their extent and severity. Indirect features like landscape may help to identify the problems of soil salinity. Relative elevation is one of the most evident landscape features in relation to salinity and moisture provided by saline and shallow groundwater table. At present, the identification and mapping of saline soil is a combination of the following:

- (i) visual interpretation of photographs
- (ii) digital analysis of false colour composite (FCC) and
- (iii) digital analysis of surface radiation and vegetation index.

All methods require ground truth information for calibration and validation. The actual use depends on the specific aim of the survey, data availability, human skill and availability of time and money.

## **2.2.1 Salt-affected Soils and Spectral properties**

### **2.2.1.1 Application at field level**

The acquisition time of the RS data is important for the identification of soil salinity. Rao and Venkataratnam (1991) used temporal Landsat-MSS images of pre-monsoon, post-monsoon and harvest seasons to map soil salinity in the State of Punjab, India and concluded that the spectral curves of highly and moderately saline soils change considerably throughout the annual cycle, which significantly complicates the time composition procedure. Johnston and Barson (1993) reviewed RS applications in Australia and found that discrimination of saline areas was most successful during peak vegetation growth. In other periods, the low fractional vegetation cover of salinized area could not be distinguished from areas that were bare due to overgrazing, erosion or ploughing. It was also found that salinity was best expressed at the end of the irrigation or rainy season, when the plots were bare. Goossens *et al.* (1998, as cited in Salman, 2000) analyzed the beginning, middle and end of the growing season in the western Nile Delta and concluded that single image may be suitable for detecting severely salinized soils but more gradations can be determined using temporal images.

IDNP (2002) reviewed studies conducted by different researchers on direct observations on bare soils and indirectly by vegetation cover. For the visible part of the spectrum, the soil reflectance of salt cover areas was found to be prominent. Bands in the middle infrared gave information of moisture content, which was often associated with salt content differences and some information on type of salts. The lack of vegetation or scattered vegetation and highly salt-affected salt surface make it possible to directly detect salt on the surface.

It is to be pointed out that reflectance in visible and infrared bands provides only information of the first millimeter of the top horizon of the bare soils. Often, the characteristics of the surface are found to be different from the layer below. Ground observations and radiometric measurements indicated that the main factors affecting the reflectance are the quantity and mineralogy of salt, moisture, colour and roughness. The evaluation of soil surface remains under the influence of external factors as groundwater quality and variation of depth, wetting/drying cycles and wind. On the contrary, pure and thick salt crust or sand deposits can be used as

calibration site for reflectance measurements. Many researcher described salinity detection through use of vegetation on the basis of the fact that reflectance from single leaf depends on their chemical composition (salt) and morphology (Moulders, 1987).

Metternicht and Zinck (1996), based upon their studies related with ground observation and radiometric measurement in the visible and near infrared wavelengths that the main factors affecting the reflectance are the quantity and mineralogy of salts together with soil moisture, soil colour and terrain roughness, which in turn are controlled by different combination of salts and type of soil surface, texture and organic matter content. Salts influenced surface features include the soil crusts with or only little evidence of the presence of the salts. The crusted soil surfaces are generally smoother than non-saline surfaces and cause higher reflectance values in the visible and near infrared bands. Apparently, the physiological status of the crop is best manifested at TM 5 and 7, while TM bands 3 and 4 are better suited to describe the overall crop development. The multiple regression analyses between SPOT spectral data and soil morphological, physical, and chemical properties showed that many surface and some subsurface soil properties were significantly correlated.

Brightness index proved to be a more useful spectral parameter if surface soil properties are to be extracted from satellite data, but ratio of the values in red and infrared band seems to be a better technique to employ when subsurface soil properties are of interest. Moulders (1987) remarked that in general, bands in the near and middle infrared region give reasonable information on soil moisture and salinity. Steven *et al.* (1992) confirmed this finding by showing that near to middle infrared index is a better indicator for chlorosis occurring in stressed crops (normalized difference for TM bands 4 and 5). This new ratio is immune to colour variations and provides an indication of leaf water potential. The spectral behaviour of salt-affected soils as compared to normal cultivated soils showed relatively higher spectral response in visible and near-infrared regions. Further, strongly saline-sodic soils were found to have higher spectral response as compared to moderately saline-sodic soils. The vegetation cover modifies the overall spectral response pattern of salt-affected soils especially in the green and red spectral bands.

Spatial resolution has significant effect on enhancing the identification of salt affected soils and crops. Landsat-MSS is of limited use to identify saline plots due to its low spatial resolution. Many researchers compared the accuracy of TM, MSS, and SPOT and found TM to be the superior multi-spectral radiometer for soil salinity mapping (Steven *et al.*, 1992). Digital classification techniques help in improving the identification and mapping of salt-affected soils or crops.

### **2.2.2 Water logging**

Excess soil moisture can cause a change in soil colour and a change in soil reflectance properties, which can be easily detected by remote sensing. Plant response is one means of detecting poorly drained soils in California mainly because of a buildup of the water table. On the other hand, due to the accumulation of organic matter, soil colour is generally darker in poorly drained areas than well drained soils (Salman, 2000).

The visible bands in Landsat- MSS data can be used to identify this colour. Baber (1982, as cited in IDNP, 2002) pointed out that colour infrared photography could indicate drainage problems by soil moisture saturation or plant stress. Shallow water tables exhibit an increase in surface moisture, which can be detected from visible reflectance and microwave emissivity.

The information about drainage basin area and drainage pattern can be obtained from satellite imagery. GIS helps in assessing water logging and drainage problem by identifying the drainage network and its characteristics in a basin, besides the information on the presence of high water table, high morphology, soil colour, plant stress and drainage water collection in lower spots.

### **2.2.3 Application to large areas**

Remote sensing is an important tool for mapping and surveying salt-affected and waterlogged soils for relatively large areas. The knowledge of the actual conditions at the earth surface makes it possible to interpret the satellite images. However, it is very difficult to distinguish the degree

of salinity through remote sensing techniques due to lack of specific absorption bands and spectral confusion. In the past, Landsat data have been used for separating different levels of soil salinity. Most authors are able to distinguish only 2- 3 classes (strong and medium) of salinity levels with errors between moderately saline and normal soils.

**2.2.3.1 Visual interpretation using photo imagery:** Evolution of the salinity begins with small and irregular bare soil patches. IDNP (2002) reviewed a study carried out for the entire Indian territory (329 m ha) using Landsat - MSS FCC of 1:1,000,000 scale and categorized wasteland as salt-affected, gullied, waterlogged or marshy, undulating upland with or without scrub, forest blank, sandy areas (coastal or desert), barren hill ridge or rock outcrops and snow covered/glacial areas. The interpretation technique was supported by intensive ground data and geographical knowledge of the area. An accuracy of 80 to 90 percent has been achieved in the identification and mapping of wastelands when compared with the ground survey. Rao and Venkataratnam (1991) used Landsat-TM standard FCC and delineated strongly sodic soils as bright white patches with fine texture, and moderately sodic soils as dull white to strong brown. Underestimating of surfaces covered with salts using remote sensing was attributed to confusion with slightly saline and non-saline soils.

Aerial photographs and Landsat-TM data could be used to monitor changes in the status of salt-affected soils. Aerial photographs on a 1:40,000 scale and standard FCC image on 1:50,000 scale provided a minimum delineation of 2 ha size. In this study, FCC enlarged on the 1:50,000 scale were visually interpreted using image interpretation elements as clues to delineate salt affected soils. Based upon the colour variation, two classes of salt-affected soils i.e., severely and moderately salt-affected soils could be distinguished. Severely salt affected soils with thick salt efflorescence on the surface appear as white patches whereas, moderately salt-affected soils appears light bluish green in colour. According to Kalra and Joshi (1997), Landsat (MSS & TM), SPOT and IRS (LISS-I & 11), FCC images during fallow period April-May, January/February crop and rain fed crop (October) were used and evaluated the capability of multi-sensor data for delineating salt-affected soils in arid Rajasthan. It was concluded that the moderately and severely salt-affected soils could be mapped from any season's FCC of Landsat, SPOT and IRS. However, the summer season images provided the maximum extent of salt-affected soils. Saline

soils due to irrigation based on peculiar tone and pattern could be mapped separately by using irrigated crop season (January) images supplemented by knowledge of the quality of irrigation water used. The differentiation between the saline and sodic soils was possible only by the use of multi-date imagery (October and January) and the clue provided by the cropping pattern.

**2.2.3.2 Digital analysis:** Remote sensing investigation on soil salinity can be divided into the delineation of salt-affected soils under:

- (i) Bare condition and
- (ii) Cropped condition.

Salinized and cropped areas can be identified with a salinity index based on greenness and brightness that describes leaf moisture as influenced by salinity, with classical false colour composites of separated bands, or with a computer assisted land surface classification (Kauth and Thomas, 1976; Steven *et al.*, 1992; Vincent *et al.*, 1996). Essentially, a brightness index is meant to detect high levels of brightness appearing at high levels of salinity. The contributive power of false colour composites and visual interpretations are demonstrated in most studies. The unique patterns of geomorphologic shapes are thought to be helpful in discriminating the salinization process from a physiographic perspective.

Based on the spectral response of these soils and subsequent correlation in the field by studying terrain characteristics and soil profiles, besides salt-affected soils, other categories such as normal soils, forests, water bodies, river sand, gullies and ravines could be mapped. Salman (2000) has reviewed application of remote sensing in contextual classifier for soil salinity mapping with a built GIS to link the location of the irrigation feeders and drainage master canals in the western Nile Delta with digital elevation data and satellite classifications. Soil salinity risks are considered to be proportional to the distance of field from the main irrigation canals, as well as to the field elevation difference with the main irrigation canals. TM bands 2, 3,4,5,6 and 7 were used to classify three different stages of water logging according to a simple supervised procedure.

**2.2.3.3 Digital analysis using surface vegetation index:** A vegetation index is a common spectral index that identifies the presence of chlorophyll. Various crop indices have been derived using the fact that chlorophyll strongly absorbs the light energy in the red part and highly reflects in the near-infrared part. Various researchers for specific analyses have proposed number of vegetation indices. Many papers described salinity detection through its impact on the vegetation. An inverse relationship is observed between reflectance and salinity, as salt content induces less plant cover (decreasing of density, LAI, and height) and some times slight salt deposition on surface associated with vegetation have similar reflectance as that of normal cropped area (Richardson *et al.*, 1976). Salt tolerant plants are good references of salinity level on salt marshes but require good calibration. Contrasted associations of vegetation and bare soils can be more useful for salinity detection than individual surface types.

Although the soil profile cannot be evaluated on remotely sensed imagery, spectral characteristics of the earth surface features that are indicative of subsurface conditions can be analyzed. Because satellite multi-spectral data denote changes that aid in locating mapping units, they hold great promise for soil surveys and land-use planning. Some relationships have been established between soil properties and spectral data. While most of these properties have been from the surface soil, subsurface properties that influence some surface characteristics were considered. Although satellite sensors observe only the ground surface, actually both surface and subsurface soil conditions are affected by common genetic factors. Both subsurface conditions and surface conditions are plant canopy. Therefore, when satellite imagery depicts a pattern based on a different spectral response, it is not unreasonable to attempt some inferences about subsurface soil patterns.

In sum, sincere but limited attempts have been made in the past to identify the water logging and soil salinity problems using remote sensing. However, most of the studies have been site specific. Apparently, methodology for identification of these problems is still lacking. Therefore, several studies were attempted to develop, within a broad framework, a methodology for diagnosis of water logging and soil.

## **2.3 GIS in Soil Salinity Modeling**

A model is a representation of reality. Due to the inherent complexity of the earth and the diverse interactions in it, models are created as a simplified, manageable view of reality. Models help understand, describe, or predict how things work in the real world. There are two types of models; those that represent the objects in the landscape (representation models) and those that attempt to simulate processes in the landscape (process models).

Representation models try to describe the objects in the landscape, such as buildings, streams, or forest. Process models attempt to describe the interaction of the objects that are modeled in the representation model. There are different types of process models including suitability modeling, distance modeling and hydrological modeling.

### **2.3.1 Soil Salinity modeling using multi-criteria decision evaluation**

Decision Theory is concerned with the logic by which one arrives at a choice between alternatives (Saaty, 1977). Those alternatives vary from problem to problem. They might be alternative actions, alternative hypotheses about a phenomenon, alternative objects to include in a set and so on. Resource allocation decisions are also prime candidates for analysis with a GIS. Indeed, land evaluation and allocation are the most fundamental activities of resource development (FAO, 1976). To meet a specific objective, several criteria are to be evaluated. Such a procedure is called Multi-Criteria Evaluation (Voogd, 1983; Carver, 1991). Multi-criteria evaluation (MCE) is most commonly achieved by one of two procedures. The first involves Boolean overlay whereby all criteria are reduced to logical statements of suitability and then combined by means of one or more logical operators such as intersection (AND) and union (OR). The second is known as weighted linear combination (WLC) wherein continuous criteria (factors) are standardized to a common numeric range, and then combined by means of a weighted average. Such a procedure is essentially risk-averse, and selects locations based on the most cautious strategy possible - a location succeeds in being chosen only if its worst quality (and therefore all qualities) passes the test.

A pair-wise comparison method has been used for the development of weights of the factors in the salt affected soil analysis. Here, breaking the information down into simple pair-wise comparisons in which only two criteria be considered at a time can greatly facilitate the weighting process, and will likely produce a more robust set of criteria weights. A pair-wise comparison method has the added advantages of providing an organized structure for group discussions and helping the decision making group one on areas of agreement and disagreement in setting criterion weights.

The technique described here and implemented in IDRISI is that of pair-wise comparisons developed by Saaty (1977) in the context of a decision making process known as the Analytical Hierarchy Process (AHP). The first introduction of this technique to a GIS application was that of Rao *et. al.* (1997), although the procedure was developed outside the GIS software using a variety of analytical resources. In the procedure for Multi-Criteria Evaluation, using a weighted linear combination outlined above, it is necessary that the weights sum to one. In Saaty's technique, weights of this nature can be derived by taking the principal eigenvector of a square reciprocal matrix of pair-wise comparisons between the criteria.

### 3. Methodology

#### 3.1 Description of the study area

Metehara sugarcane estate is located 190 km southeast of Addis Ababa near Metehara town in Fentale Woreda, Oromia region, East Central Ethiopia between 08°35'N and 08°54'N latitude and 39°40'E and 39°55'E longitude (Figure 3.1). Metehara sugarcane estate has Abadir and Metehara farms are located at the southern and eastern side of the lake Beseka, respectively. The volume of this lake is increasingly high ever since Metehara Sugarcane farm was founded where area of the water has risen from 5 km<sup>2</sup> in 1960's to 40 km<sup>2</sup> in 1998. According to Booker (2008), the lake has posed salinity problems in Metehara sugarcane farm, blocked livestock drinking points, inundated 160 ha of land from Metehara Sugar Factory(MSF), forced Ethiopian Road Authority(ERA) to raise level of the road, and inundated 35 sq km of grazing land and also created fear of inundation among the residents of Metehara town.

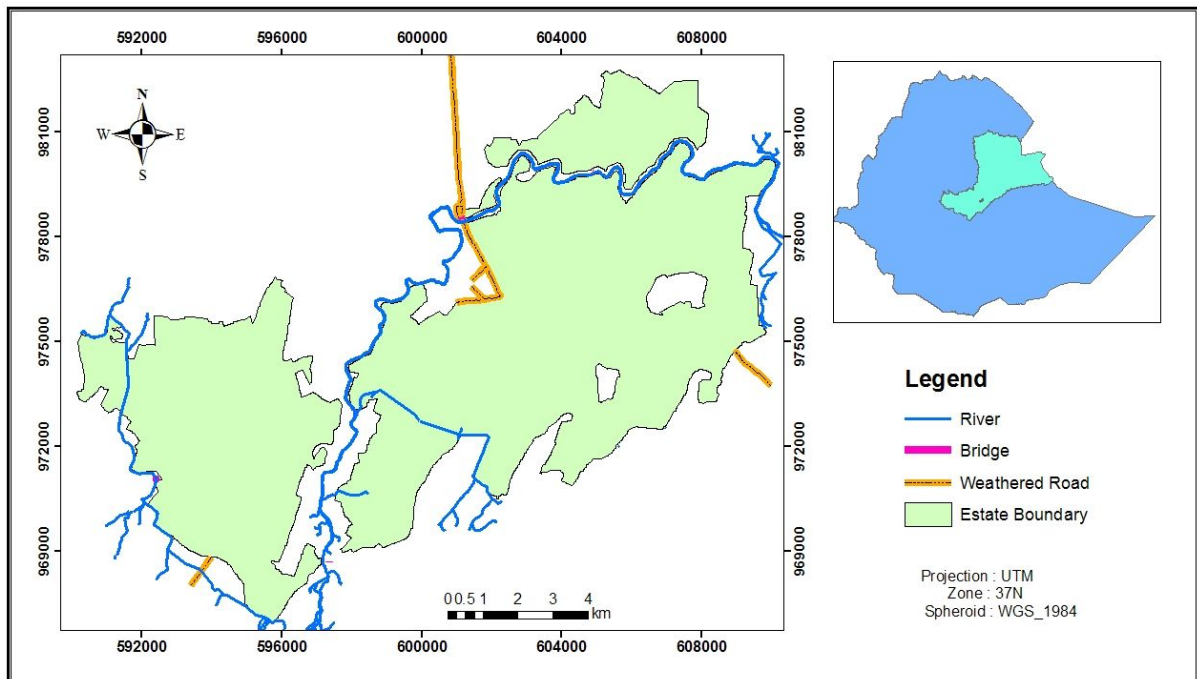


Figure 3.1 Location map of the study area.

The main cause of the increasing the volume of this lake is believed to be the blockage of the natural waterway downstream in the holdings of Metehara Sugarcane farm.

### 3.1.1 Climate

The study area falls within the traditional Kolla agro-climatic zone, which can be classified as semi-arid tropical lowland climate. According to climatic classification developed in the Agro-ecological Zones of Ethiopia, the study area has a warm to hot (22 to 29 °C) thermal zone and semi-arid moisture zone (40 to 60 days of length of growing period), termed as hot to warm semi-arid lakes and Rift valley (MoWR, 1999).

The nearest meteorological station to the study area is at Metehara. The study area has a unimodal rainfall pattern, with the rains highly concentrated between July and September, during which more than 50% of the annual rainfall is received. The mean annual rainfall is around 540mm. Smaller peaks occur in April. The mean annual temperature at Metehara is 26 °C and monthly mean values range between 23 °C (in November) and 29.2 °C (in June). The mean annual free water evaporation as recorded by the class A pan is around 1903 mm. As a result of this, the soil is dry for a longer period. This hinders any great leaching of soluble salts or complete leaching of the salts (Table 3.1).

Table 3.1. Meteorological data of Metehara town.

Element	Jan	Feb	Mar	Apr	May	June	July	Aug	Sep	Oct	Nov	Dec	Annual
T <sub>min</sub> (°C)	14	17	18.6	19	19.2	22.1	20.2	19.7	19	16	14	14	18
T <sub>max</sub> (°C)	31	32	34.2	34	35.6	36.3	33.1	32.3	34	34	32	31	33
T <sub>avg</sub> (°C)	23	25	26.4	27	27.4	29.2	26.7	26	26	25	23	23	26
Humidity (%)	59	60	57	57	52	50	59	63	58	53	54	57	57
Wind(m/sec)	1.6	1.7	1.6	1.4	1.4	2	2.2	1.7	1.3	1.3	1.4	1.4	2
Sun shine (hr)	9	8.7	8.5	8.4	8.8	8.7	7.4	7.4	7.7	8.7	9.4	9.4	9
ETo(mm)	146	143	171	162	174	186	171	158	150	158	144	140	1903

### **3.1.2 Geomorphology, Soil and Parent Material**

The study area consists of two major geologic formations; Tertiary and Quaternary volcanic of the Ethiopian Rift System, composed predominantly of volcanic materials such as rhyolitic lava, pumice and tuff (MoWR, 1999). The study area occupies a down-faulted almost a closed basin (with two major NE-SW oriented step-faults) that has been filled up by volcanic materials (predominantly pumiceous alluvium) imported by the seasonal streams from the adjacent hills and mountains (Fentale Mountain) and the Rift Valley escarpments in the west. On the margins of the basin, adjacent to hills, ridges and mountains, occurs coarse alluvial/colluvial material deposited over the pumiceous alluvia.

The parent material of the soils may be grouped as volcanic materials, general skeletal soils of ancient alluvial and lacustrine sediment, varying in phase: fine, saline, sodic and recently deposited alluvium at the Rift Valley depressions adjacent to Awash River. The soil of the study area is predominantly Calcaric, Vertic and Hypovertic Cambisols. Soils are generally heavier in texture and patches of the original state were Saline / Alkaline. The newly developed areas at Metehara, particularly in the lake area were reported as highly saline or alkaline (OWWDSA, 2007).

## **3.2 Methods**

The work consists of Remote sensing analysis, GIS assisted spatial modeling and regression analysis.

### **3.2.1 Salinity Indices**

In order to enhance the saline zones and suppressing the vegetation, two indices: Salinity Index (SI) and Normalized Difference Salinity Index (NDSI) were proposed in this study. SI is the ratio of red band to near infrared (NIR) band while NDSI is the ratio of the difference of the red to NIR and divided by the summation of the two. This concept has emerged from the Red Edge concept for vegetation vigour mapping. In red edge concept, the spectral reflectance of NIR is radioed with red band, which gives very high values for vegetation than other features on Earth. Here if the inverse is considered, then for vegetation low values will be obtained, thus suppressing the vegetation and highlighting the soil. SI and NDSI are computed as follows:

$$SI = (\text{Band 3} / \text{Band 4})$$

$$NDSI = [(\text{Band 3} - \text{Band 4}) / (\text{Band 3} + \text{Band 4})]$$

### **3.2.2 Vegetation Indicator**

Salt affected soils are usually characterized by areas of poorly developed vegetation and such state of stressed vegetation could be an indirect sign of the presence of salts in the soils. A vegetation index is therefore included in the analysis as:

$$\text{Normalized differential vegetation index: } NDVI = [(\text{Band4} - \text{Band3}) / (\text{Band3} + \text{Band4})]$$

### 3.2.3 Empirical Models of Soil Salinity and Spectral Reflectance

The procedure employed was by identification of the location of sampling point sources on satellite data. The corresponding reflectance of soil samples from different sampling zones were retrieved for different bands and indices. An empirical model for NDSI vs salinity level (EC) was prepared using regression analysis (Figure 3.2).

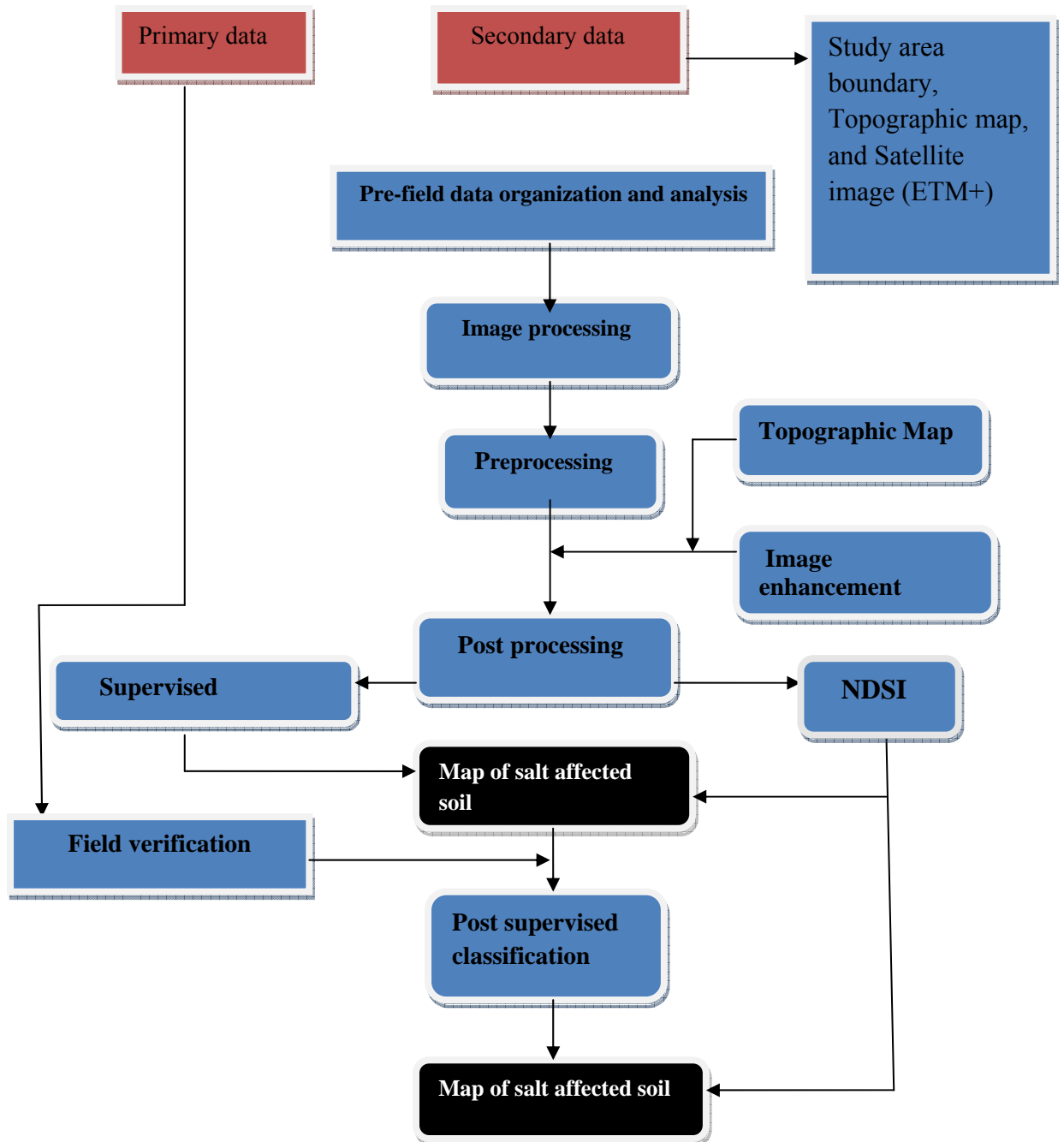


Figure 3.2. Classification of salt affected areas by satellite imagery.

### 3.2.4 Overlay Soil Salinization Model

A model of salinity development was formulated upon the interaction of the factors. As a result to determine the spatial soil salinity potential for the Metehara irrigated land, it can be formulated by coupling a GIS to additional model relating the interaction of four thematic layers: geologic formation, ground water level, landform and land cover (Figure 3.3).

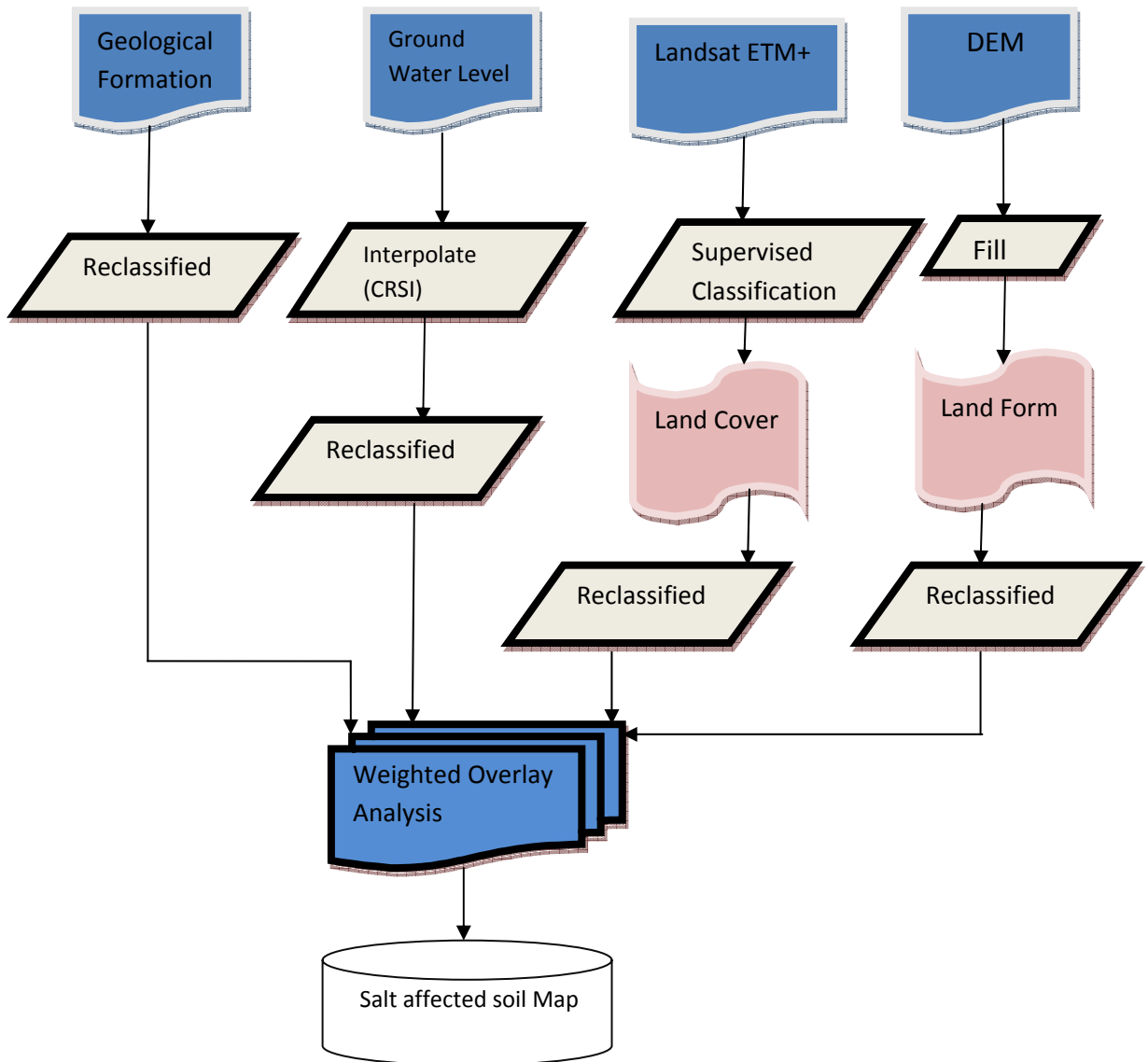


Figure 3.3. Classification of the salt affected areas based on geology, land form, ground water level and land cover.

The build up of salt in the soil surface is basically found on the land, which is underlain by the geology of the area. Saline soils of Metehara estate were reported as natural due to volcanic

activity and the climate and possibly from the original residual (lacustrine) effects of the lake. There are still few such areas in the original estate. The ground water level greatly enhances the salinization of soil (Girume Bekele, 2005). Shallow water tables are recognized to be influential in the development of soil salinity as a result of the high potential for upward movement of soluble salts. In addition, the areas under vegetation cover decreased salt accumulation at the soil surface while the surrounding areas with bare land are likely to result in higher salinity. The accumulation of salt near the soil surface, due to the upward movement of salt carries by the water rising and the lateral movement is highly related to the low terrace (Mongkolsawat and Thirangoon, 1990). As a result, the soil salinization model in Metehara estate is then based on the interaction of geology, ground water level, land form and land cover.

Applying the model to the four factor databases the overlay operation was digitally performed to create the map units that were subsequently assigned to the soil salinity potential class. In the process of the formulation of the model, reclassification was made to adjust the conditions, which are highly correlated to the ground truth and the existing electrical conductivity of the soil. The schematic map overlaying of salinization factors as shown in Figure 3.3 in which the soil salinity map was created.

### 3.2.5 Overlay Analysis

After the salt affected areas were identified, attempts were made to assess their spatial distribution in relation to the following factors (Figure 3.4):

- Canal
- Drainage
- Water table
- Soil type

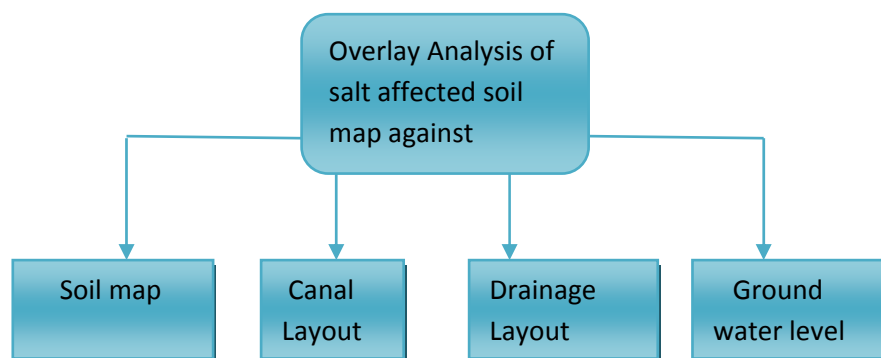


Figure 3.4. Overlay analysis of salinity map against soil map, canal layout, drainage layout and ground water level.

### **3.2.6 Spatial Data analysis**

Spatial data analysis in GIS ranges from simple mapping to creating complex spatial models. A model is a representation of reality used to simulate a process, predict an outcome, or analyze a problem.

#### **3.2.6.1 Data collection**

More than 90 sample sites were collected as it was difficult to identify all the land-use land-cover classes only by interpreting satellite images. These ground control points were used as field verification points during image classifications. Salt affected areas were clearly identified from other features by higher reflectance in many bands. However, it was difficult to differentiate salt affected area from sand soils. Therefore, sample sites that were identified as salt affected were used for image analysis, followed by model site verification.

DEM of the study area were obtained from 30 m resolution SRTM data. The satellite image ETM + 2005 was acquired. Topographic maps, 1: 50,000, that were used in digitizing thematic layers for the overly analysis. Soil map, 1:10,000 and geology map, 1:250,000 of the area were obtained from General Integrated Rural Development Consultancy PLC and Geological Survey of Ethiopia, respectively.

### **3.2.7 Classification of salt affected areas using satellite image analysis**

#### **3.2.7.1 Band Selection**

In this research, band selection was done through the analyses of reflectance properties of features, correlation matrix of the bands and spectral reflectance curve of known features in all bands. Spectral profile was generated from the image using ERDAS IMAGINE 9.1.

### 3.2.7.2 Analyses of the Correlation Matrix

Satellite data show a degree of spectral bands correlation, when the spectral values in one band are high the values in another band are expected to be high as well. The correlation matrix of the spectral bands contains useful information about the redundancy of information and selection of optimal band combination for interpretation purpose. If the bands show strong correlation (value near to 1.0), this indicates that the bands usually contain similar information. When those bands are visualized, the minimum interpretability among different feature would be noticed. Table 3.2 represents the correlation matrix of the sub-scene that was clipped by the study area boundary.

Table 3.2. Correlation matrix of bands.

	<b>Band1</b>	<b>Band2</b>	<b>Band3</b>	<b>Band4</b>	<b>Band5</b>	<b>Band7</b>
<b>Band1</b>	1.00000	0.99713	-0.29222	0.93629	0.98498	0.91769
<b>Band2</b>	0.99713	1.00000	-0.28643	0.94225	0.98661	0.91505
<b>Band3</b>	-0.29222	-0.28643	1.00000	-0.36977	-0.25470	-0.15127
<b>Band4</b>	0.93629	0.94225	-0.36977	1.00000	0.90765	0.75433
<b>Band5</b>	0.98498	0.98661	-0.25470	0.90765	1.00000	0.95636
<b>Band7</b>	0.91769	0.91505	-0.15127	0.75433	0.95636	1.00000

### 3.2.7.3 Spectral Classes of Saline Soils

The spectral reflectance of soil is governed by many factors. In the present study, the area was relatively homogenous in terms of topography, surface soil colour, texture, mineralogy and agricultural practices. The only major difference was soil chemistry, expressed in the form of surface accumulated salts. A substantial increase in the spectral response of salt-affected soils was noted. The spectral value of salt-affected soils was substantially higher than the normal soils in all the bands (Figure. 3.5).

It was observed that saline soils and harvested dry soil have similar spectral response in band 5 but a significant increase in spectral reflectance was observed in case of saline soils as compared to harvested dry soils in band 3 and band 4. This observation was extremely useful as it helps the segregation of saline soils from harvested dry soil, which was important from the reclamation point of view.

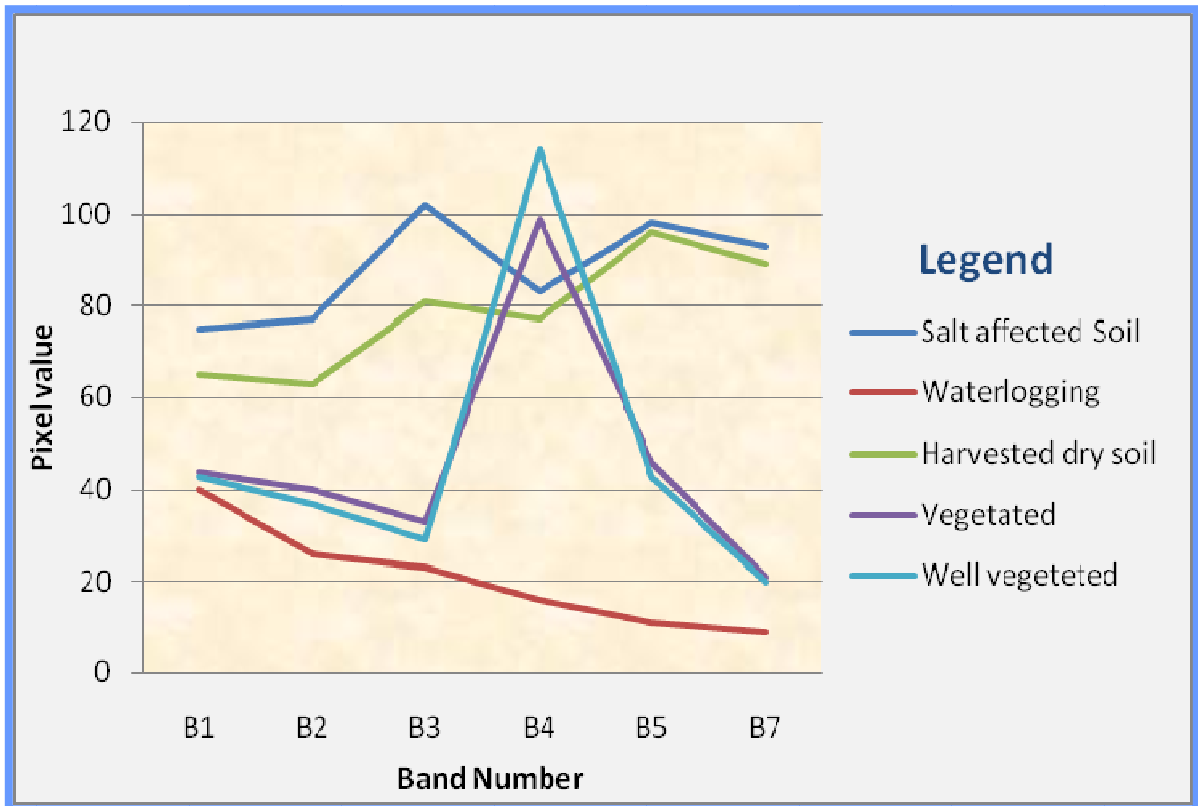


Figure 3.5. Spectral signatures of Metehara sugarcane Estate during May 2005.

### 3.2.8 True and False Colour Composite Image Preparation

To enhance the visualization of the salt affected area and to prepare the image for the future classification, various false colour composite were made. In this study, TCC and three FCC were found to be more useful for the process of discriminating different features in the study area. The different True and FCC band combinations used in this research were TCC, FCC-1, FCC-2 and

FCC-3 of ETM+ 3-2-1, 4-3-2, 3-4-2 & 4-5-3. The best image combination used for salt affected soil identification and current land-use status mapping were the TCC prepared using bands 3, 2,1 (RGB) ( Figure 3.6).

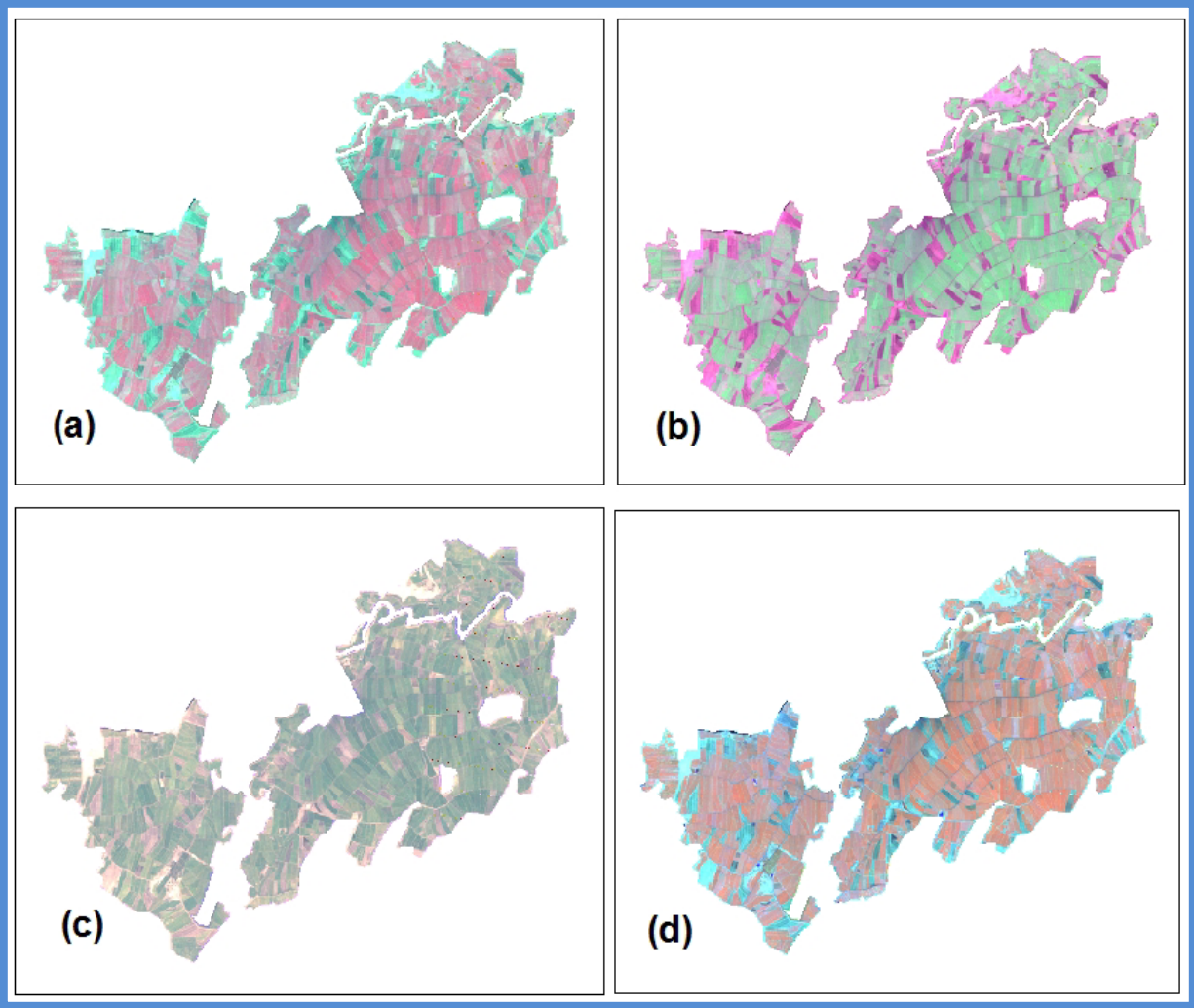


Figure 3.6. Different Landsat ETM+ band combinations: (a) combination of band 4, band 3 and band 2; (b) Combination of band 3, band 4 and band 2; (c) combination of band 3, band 2 and band 1; (d) combination of band 4, band 5 and band 3.

### 3.2.9 Spatial Distribution of ECe

An attempt was made to predict the salinity level at different locations from a number of point observations. A total of 152 EC values from a known points locations were used (Table 3.3 and see Appendix-I).

Table 3.3. EC, pH and water table for Metehara Sugarcane Estate.

Item	EC(dS/m)	pH	Water table(m)		
			April	May	June
Minimum	0.2	4.5	0.55	0.35	0.30
Maximum	103	10.8	10.8	11.85	13.4
Average	2.671128	8.6	6.21	5.34	5.28
Standard deviation	5.17133	0.57	4.125	3.829	3.758

The total number for EC/pH and Water table are 152 and 37, respectively, on predicted values calculated using various interpolation techniques. (Source of EC/pH is Generation Integrated Rural Development Consultant (GIRDC) (2005) unpublished and Piezometric data from Metehara Sugar Factory).

The locations of the EC values used were spatially distributed evenly all over the study area (Figure 3.7). The procedure employed to predict the salinity level at unsampled locations was using the scatter plot of point locations of EC vs the corresponding raster values of NDSI map extracted using ArcGIS Spatial Analyst Extension (Extract values to points). Based on the scatter plot, the best fit line which can model the interdependence of EC and NDSI raster value was determined.

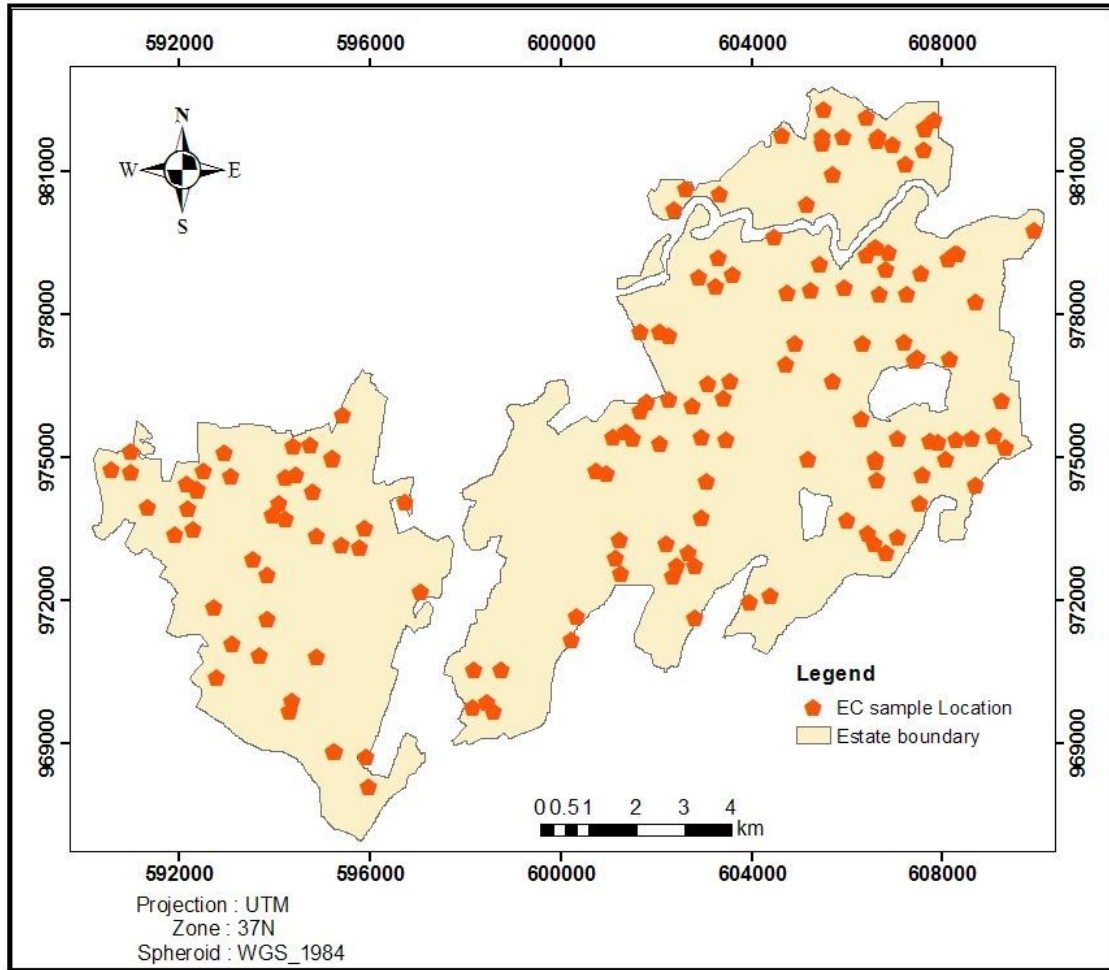


Figure 3.7. EC sample Locations.

(Source: *Generation Integrated Rural Development Consultant (GIRDC) (2005) unpublished*).

The approach used involved integrating RS data, GIS, and spatial analysis to predict soil salinity.

1. The field locations of the sampled soil salinity used was retrieved from farm plot centers (the EC values used were representative of single farm plot) and a point map was generated.
2. The location of the soil salinity data used was tied to the corresponding points on the image.
  - The soil salinity data were tested against the band 3 and band 4 as well as the normalized difference vegetation index (NDVI) and Normalized Difference Salinity Index (NDSI)
  - The EC value and the corresponding raster value were plotted on a scatter diagram and the best fit line and equation was determined.

The regression analysis between the EC values and the corresponding raster value has shown in relation with  $R^2$  of 77.5%. Based on this relation, a regression model was formulated. Figure 3.8 shows the scatter diagram and the fit plot line.

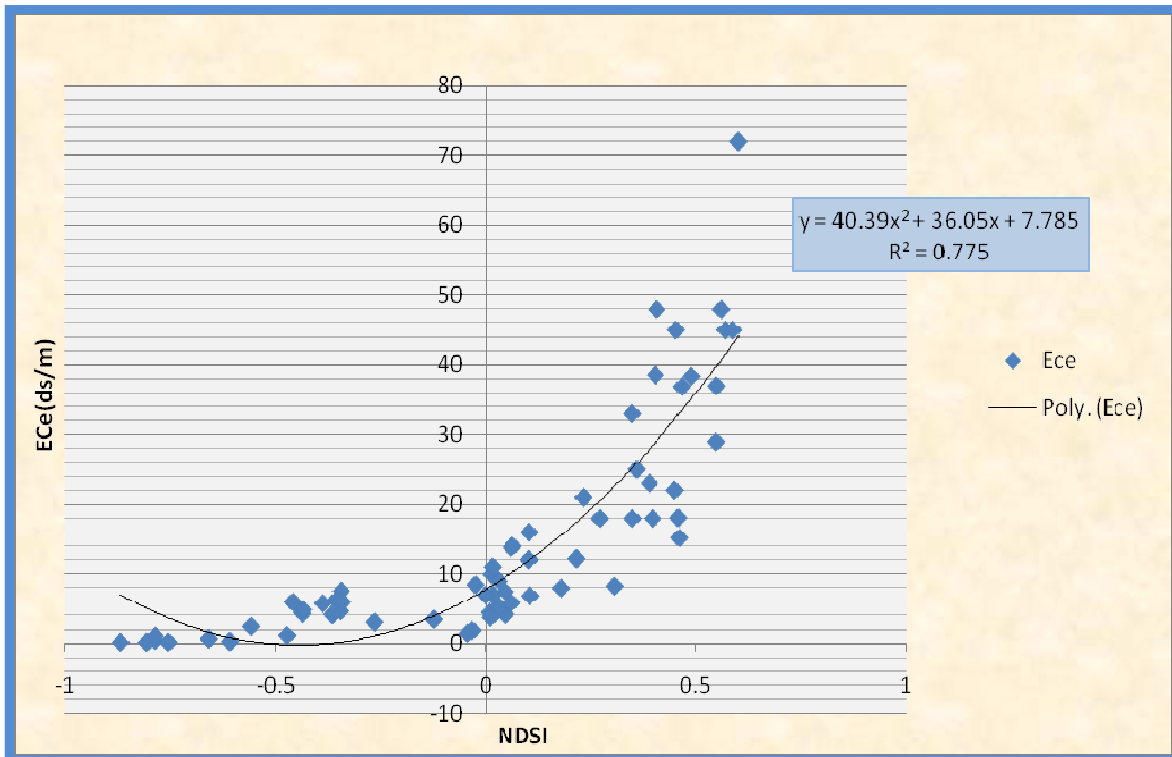


Figure 3.8. Regression Analyses between Ece and NDSI.

Based on this regression model, a raster map that predict soil salinity for all of the study area was generated using the model builder in ArcGIS (Figure 3.9)

$$\text{Salinity} = 40.39 X^2 + 36.05X + 7.785$$

Where,  $X$  represents the raster value of NDSI map

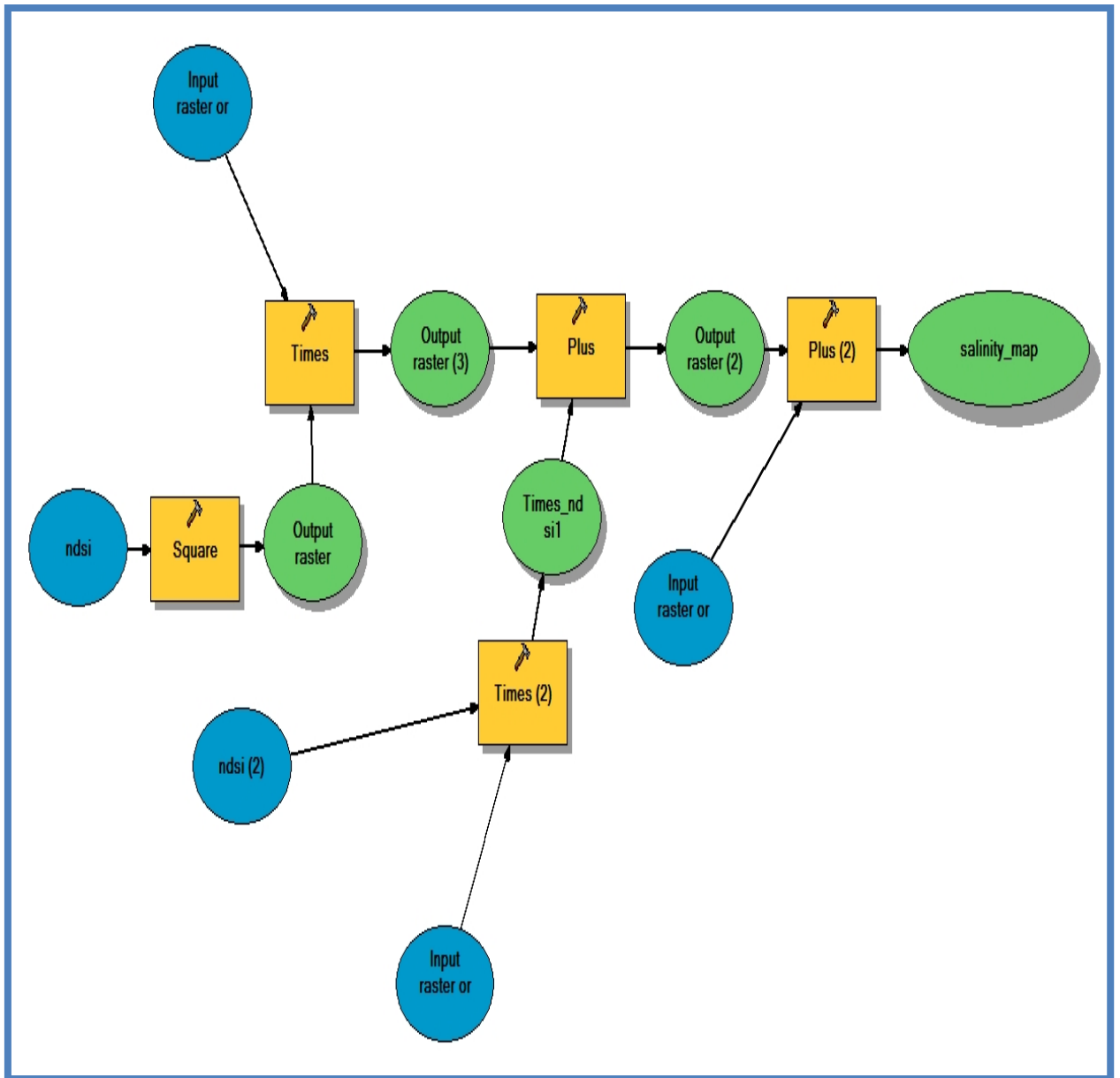


Figure 3.9. The model used for prediction of soil salinity.

### **3.3 Overlay Soil Salinity Model Analysis**

#### **3.3.1 Salinity Modeling**

Soil Salinity Modeling is a methodology or a set of analytical procedures that simulate real world conditions within a GIS using their spatial relationships of geographic features to locate the problem of salinity geographic areas for a specific land-use. Hereunder, two of the GIS functionalities are applied. Under the present study, the spatial modeling functions implemented was geometric modeling and coincidence modeling functions. Geometric Modeling Functions include calculating distances, generation buffers and calculating areas and perimeters. Coincidence Modeling Functions include overlaying datasets to find places, where values coincide. Thus, it was possible in a GIS to efficiently perform the above mentioned analysis that would be impossible or extremely time consuming if done manually.

#### **3.3.2 Model Parameters**

In running the soil salinity model the model parameters used were: ground water level, geological formation, land form and land-cover. Before the model parameters were merged to the weighted overlay analysis, the input model parameters were first converted in to a raster data model. During the conversion of the vector data in to a raster to make the data layers compatible for the raster analysis, a 30 m cell size was taken on the basis of the DEM (Digital Elevation Model) and Landsat ETM+ resolution. Therefore, all the input parameters were resampled to 30 m raster cell size resolution. In addition, to make the parameters in to a uniform scale value for the overlay analysis, each parameter was reclassified in to three salinity classes ranging from 1 to 3 on the basis of their contribution to the salinity model objective, where 1 implies least contributor, while 3 represents the most contributor part of the study area.

**a) Digital Elevation Model (DEM)**

Digital Elevation Model (DEM) of the Metehara sugarcane estate is clipped from SRTM of 30 m resolution of Ethiopian Rift valley by using a masking layer of the Metehara Sugarcane estate. The DEM shows an elevation range of very low altitude 943meter and peaks of up to 1016 meter above sea level (Figure 3.10).

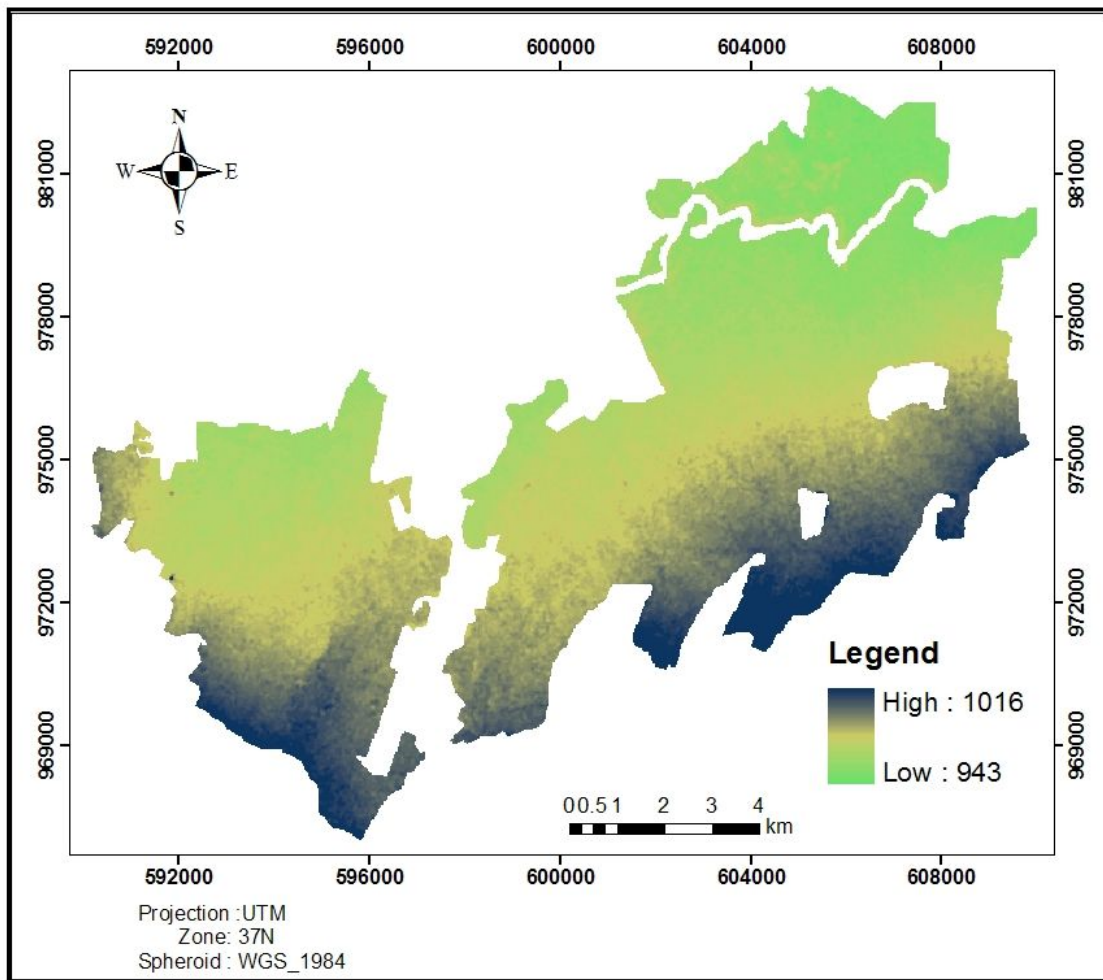


Figure 3.10. Digital elevation model of Metehara Sugarcane estate.

## b) Land form

Landforms are natural features of the landscape or natural physical features of the earth's surface. This is derived from DEM of the study area in a GIS platform using surface analysis in ArcGIS 9.2 software. The resulting land form (Figure 3.11) was derived from digital elevation model of the Metehara estate, which comprised upper and lower terraces (a leveled surface).

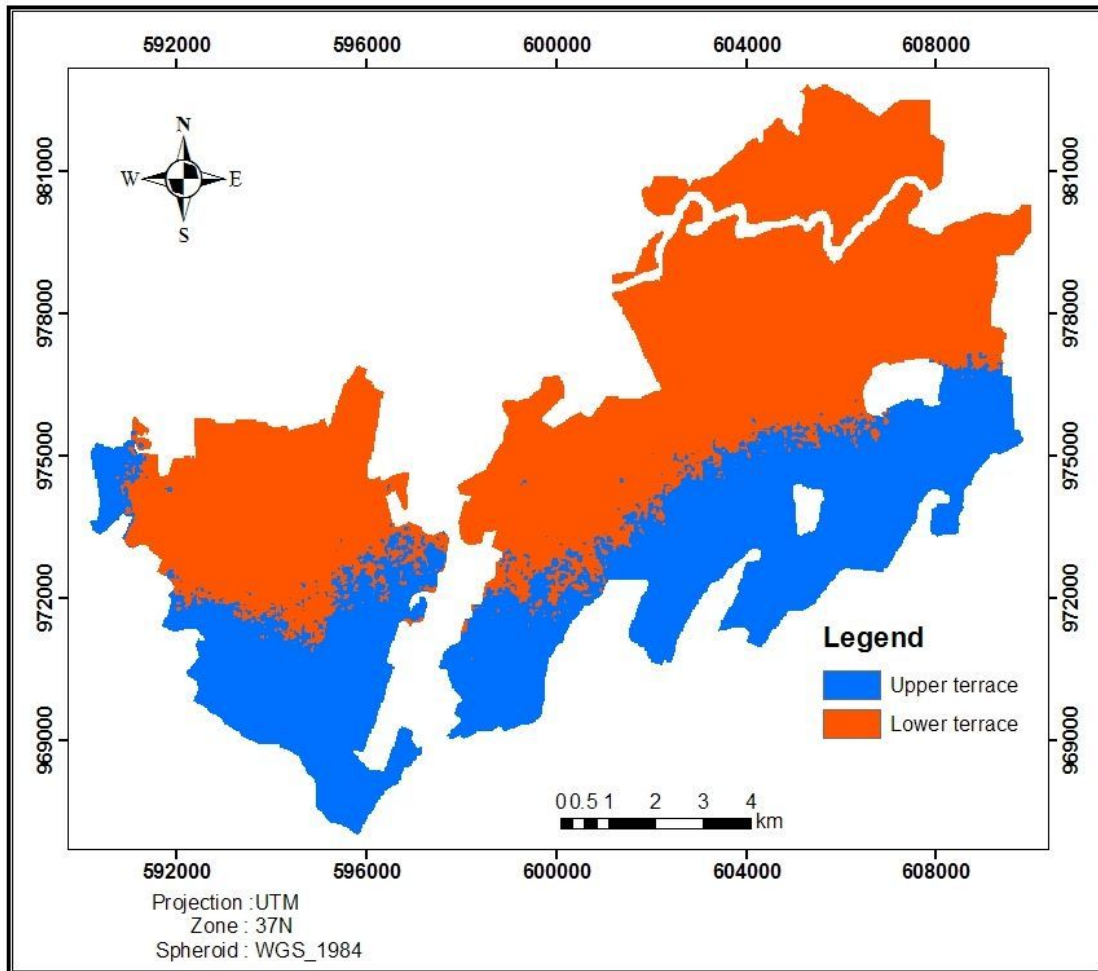


Figure 3.11. Land form of Metehara Sugar cane estate.

This value was again reclassified into two classes to make the land form compatible in the salinity modeling with other model parameters. Reclassification was involved assigning higher or lower values to more vulnerable for salinity locations, or cell values. In this study, the lower terrace land form values were those that represented higher salinity area. Since the range of the

new reclassified value was 1-3, 3 was the most vulnerable and 1 was the least vulnerable land form (Figure 3.12).

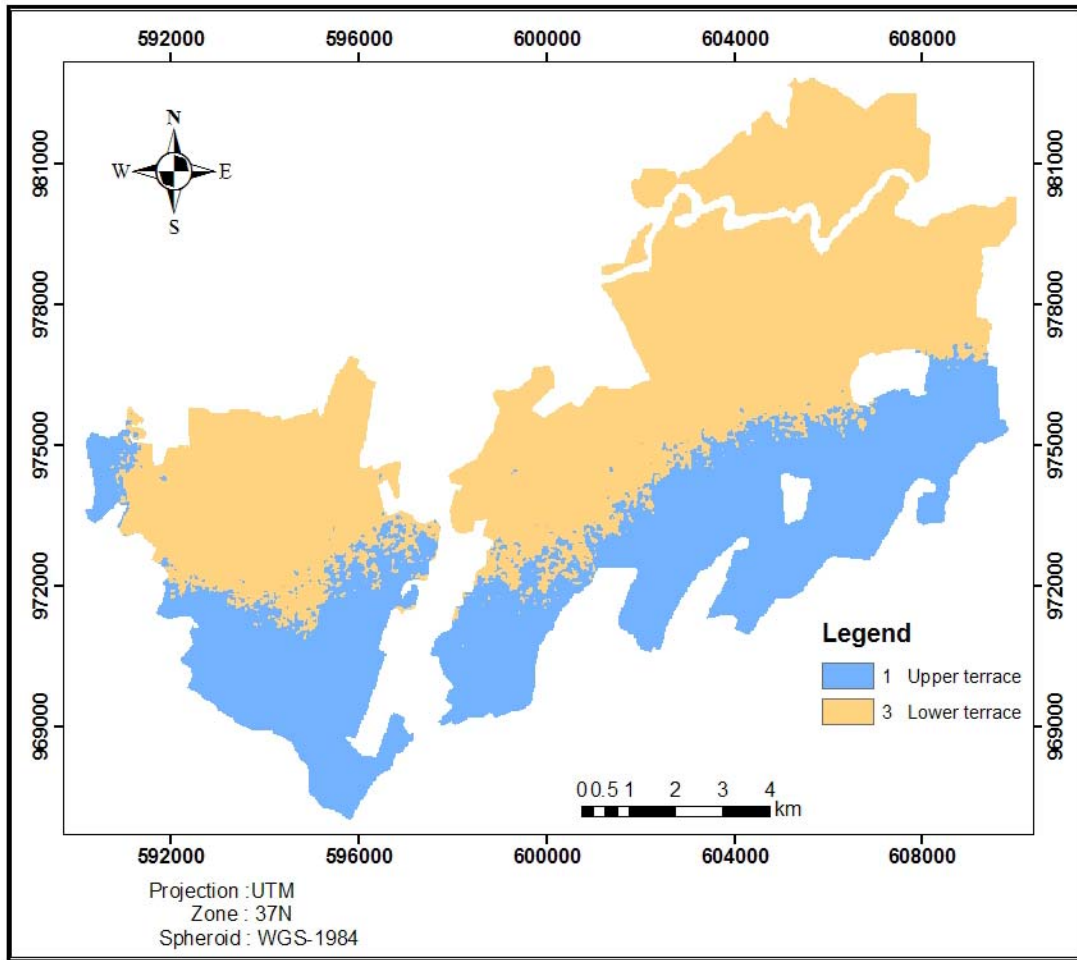


Figure 3.12. Reclassified Land form of Metehara Sugarcane estate.

### c) Land-Cover

The land cover was taken as one of the major parameters that affected the salinity modeling in the present study area. Land covers, “is the physical state of the land surface as in cropland, mountains, or forests” (Meyer, 1995). The term originally referred to the type of vegetation that covered the land surface, but has broadened subsequently to include human structures, such as buildings or pavement, and other aspects of the physical environment, such as soils, biodiversity, and surface and ground water.

The land-cover maps, based on vegetation density were prepared using Landsat ETM+ data taken in May 2005. As these salt affected soils were usually characterized by poor vegetation developed areas and such state of stressed vegetation could be an indirect sign of the presence of salts in the soil. Vegetation indices were, therefore, included in classifying land cover layer (Nasir *et al.*, 2001). The vegetation density was visually and using NDVI estimated by the geo-referenced Landsat ETM+ data to establish the land-cover. This was categorized into three classes of density: sparse, moderate and dense (Figure 3.13).

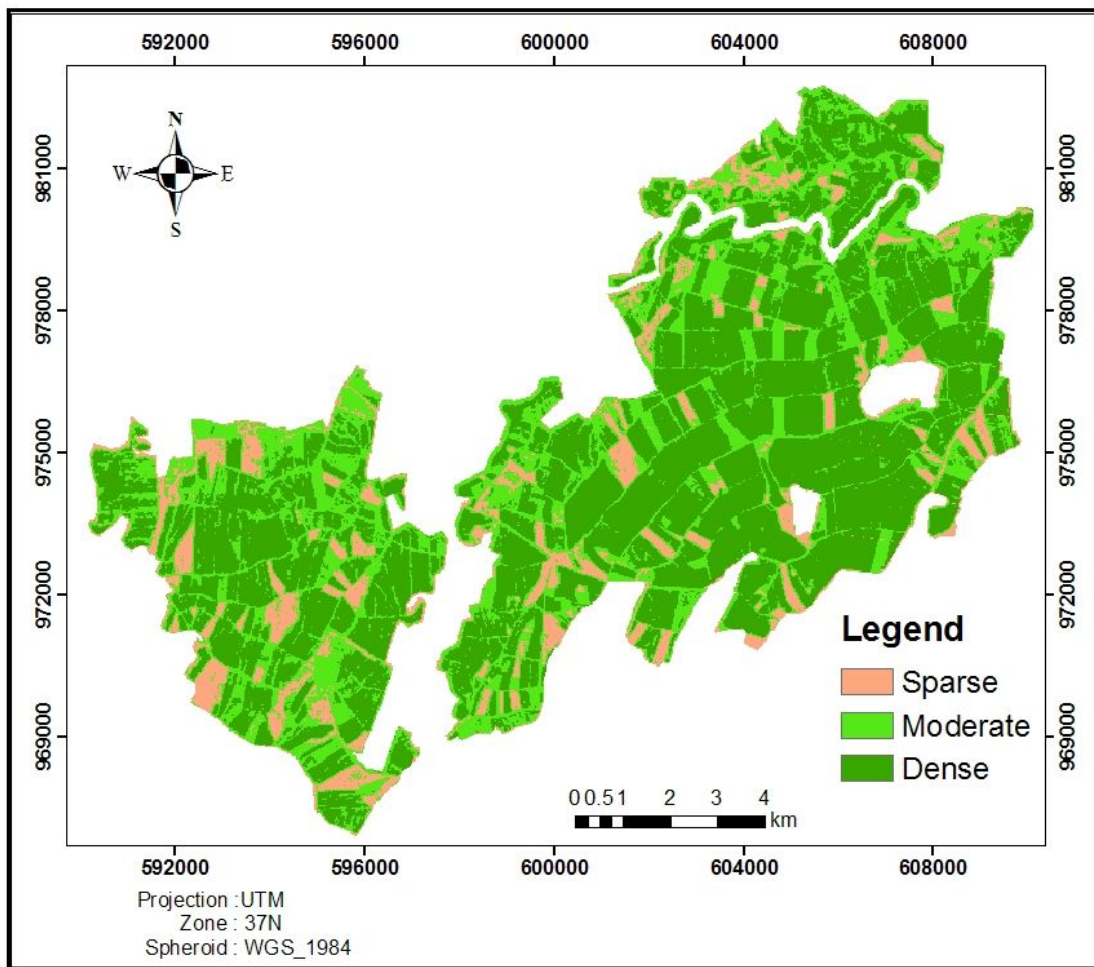


Figure 3.13. Land-cover of Metehara Sugarcane estate.

The land-cover layer was reclassified to make the parameter compatible for GIS analysis in the salinity model with other model parameters. Figure 3.14 depicts the reclassified version. Thus, the reclassified version implies 1 to 3, where 1 stands for the least indicator to salinity and 3 for the class that indicates more salinity of the soil.

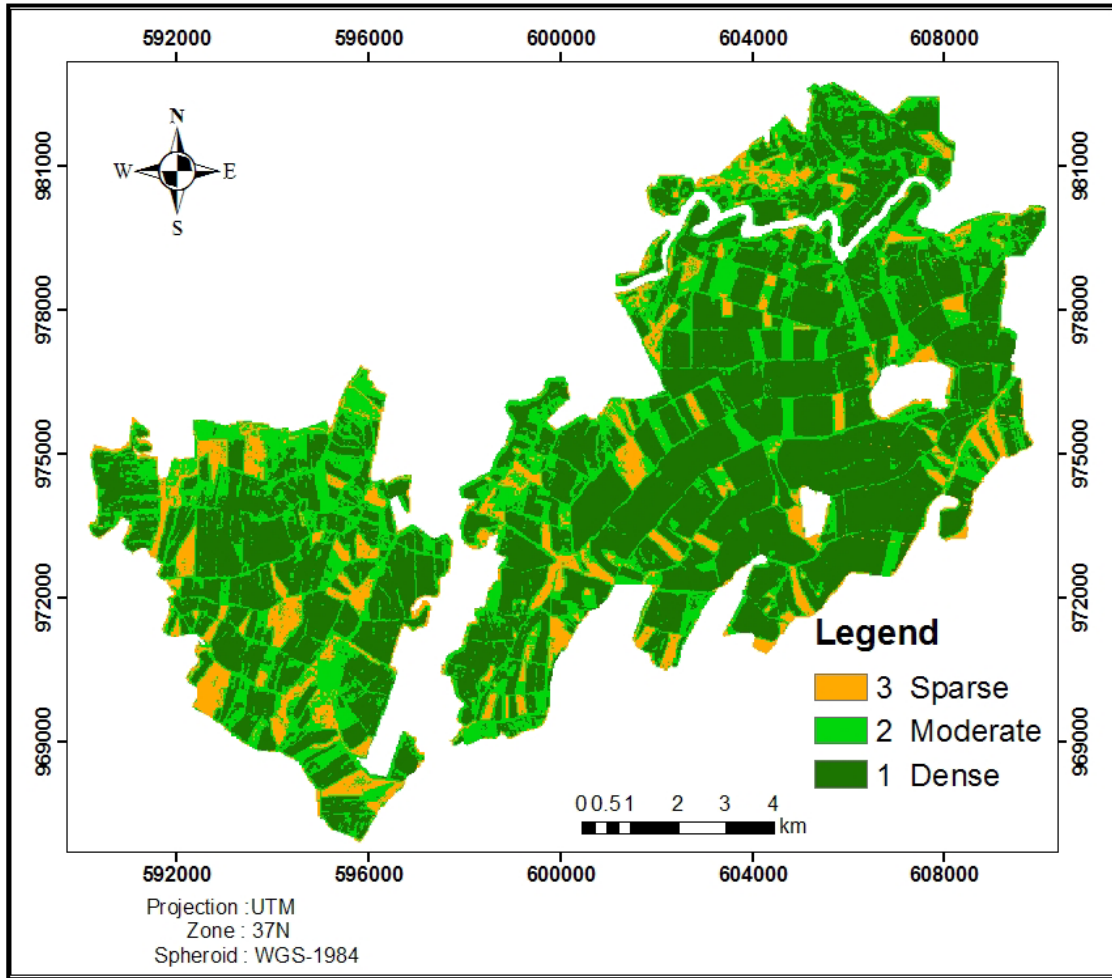


Figure 3.14. Reclassified Land-cover of Metehara Sugarcane estate.

#### d) Geological map

Geological data were obtained by digitalizing on screen one scanned official map sheets covering the study area. This geologic map developed by Institute of Geological Surveys (1978) at 1:250,000 scales was digitally encoded in the GIS database. There are three types of geological formation on the study area namely, lacustrine sediment, Pleistocene-subrecent basalts and alluvium (Quaternary sediment). The lacustrine deposits were of purely lake or swamp deposits or those of volcano lacustrine type of the rift valley. The most extensive lacustrine sediments were located around existing lakes, because they were deposited when these lakes were much larger during the pluvial times. According to Tamiru Alemayehu (2006), Salinity and high fluoride content in the rift valley was the main problems in developing groundwater in lacustrine sediments. The lacustrine sediments were situated in low-lying areas and they store

large quantities of saline groundwater. Groundwaters in the basaltic formation are known to have low concentration of fluoride as it has been found. For example, in the Bishoftu area, it was 0.3 - 1.8 mg/l. Hence, it was possible to hypothesise that even in the other parts of the Rift, groundwater in the basaltic aquifers would have low fluoride content. High fluoride content of the groundwater in the Rift was related with high salinity and alkaline environment, where it favours high concentration of fluoride in the water (Ashley and Burley, 1994). In fact, the substitution of fluoride by hydroxyl ions took place effectively in high pH waters (Mohr, 1971). Therefore, lacustrine sediments were contributing salinity to soil higher than the rest of geological formation in Metehara area. Alluvium (quaternary sediment) was moderately contributing salinity where as Pleistocene-subrecent basalts contribute least (Figure 3.15).

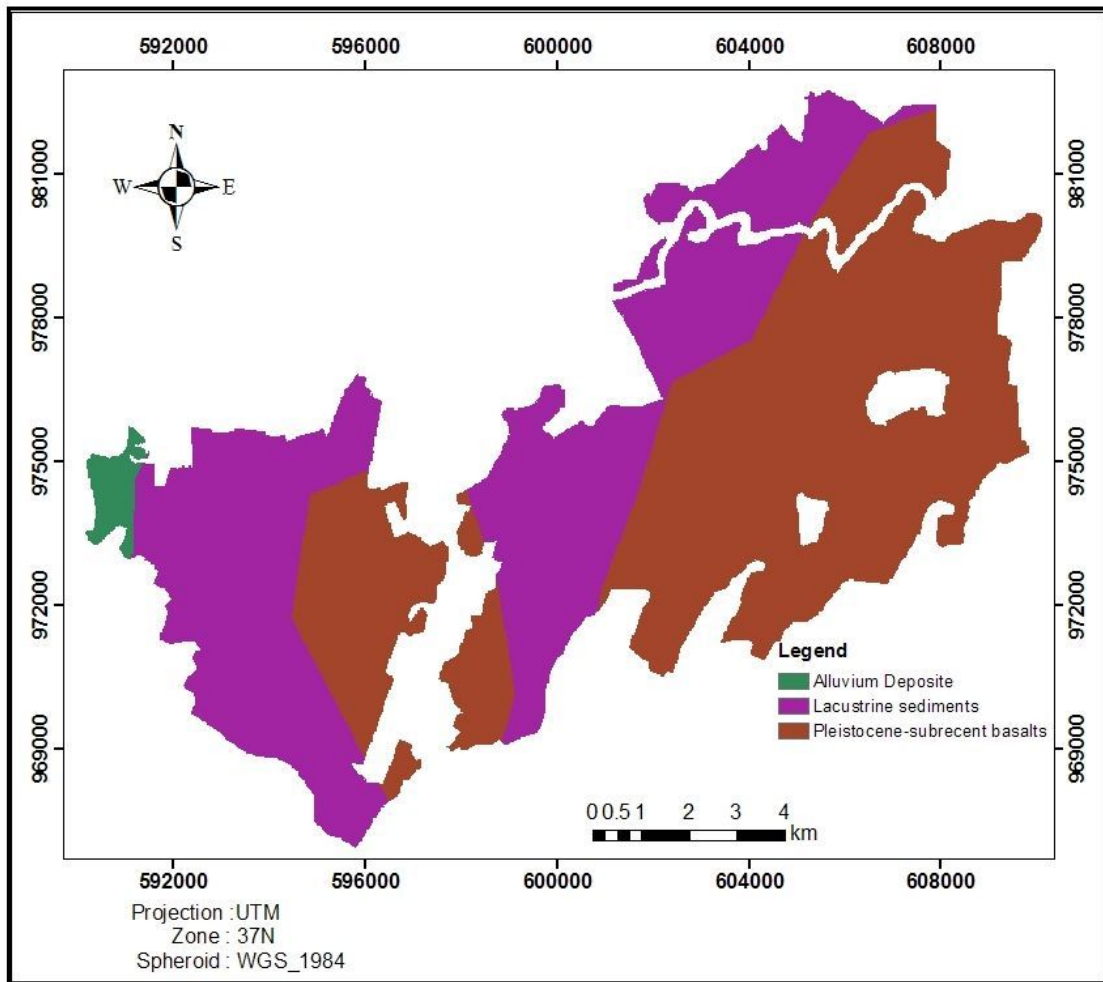


Figure 3.15. Geology of Metehara Sugarcane estate.

The geological formation layer was reclassified to make the parameter compatible for GIS analysis in the salinity model with other model parameters. Thus, the reclassified version implies 1 to 3; where 1 stands for the least contributor to salinity and 3 for the class that highly contribute the salinity of the soil with a grid map of 30m-cell size (Figure 3.16).

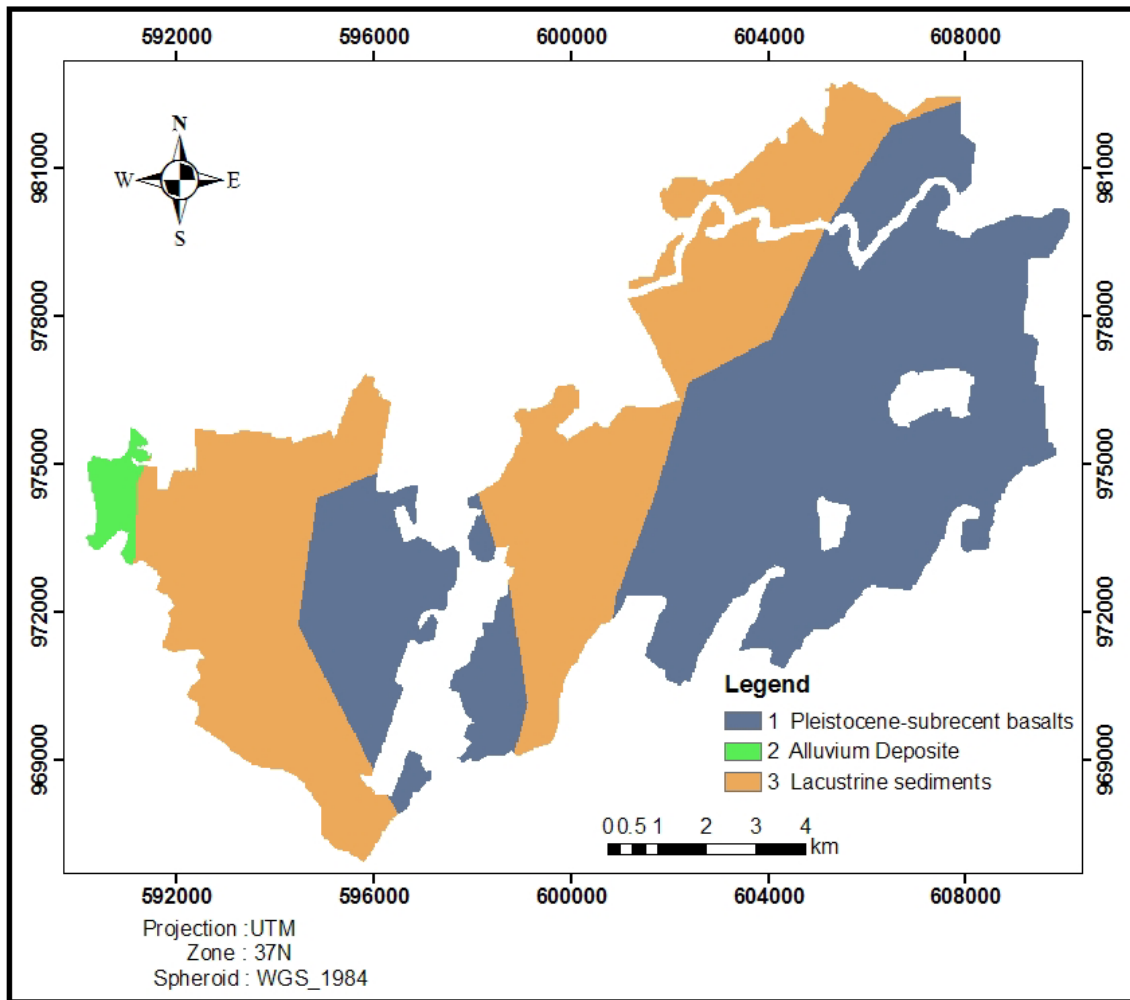


Figure 3.16. Reclassified geology of Metehara Sugarcane estate.

### e) Ground Water level

The ground water level data acquired in tabular format from department of agricultural research office in Metehara Sugar factory that has been collected in 2005 were converted in to point data in GIS environment. For ground water depths, 37 wells and piezometers were considered (Figure 3.17 and see Appendix-II).

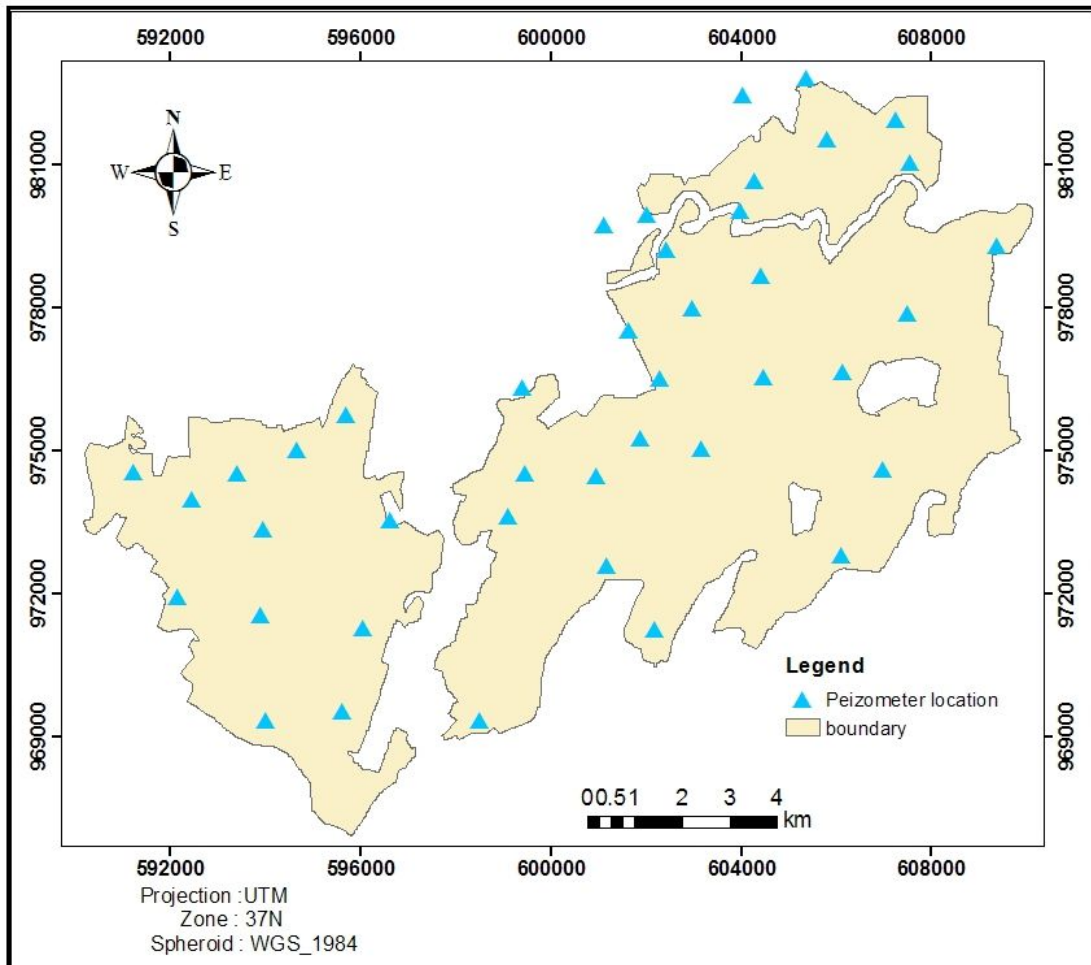


Figure 3.17. Location of Piezometric data.

(Source: *Metehara Sugar Factory*)

In order to have areal distribution of ground water level, various geostatistical methods (completely regularized spline interpolation (CRSI), inverse distance weighting, Radial basis functions and kriging) were tested. CRSI that has the lowest root-mean-square prediction error when performing cross-validation was adopted. Indeed, the smaller the root-mean-square

prediction error, the closer the prediction is to their true values and better is the interpolation method (Figure 3.18).

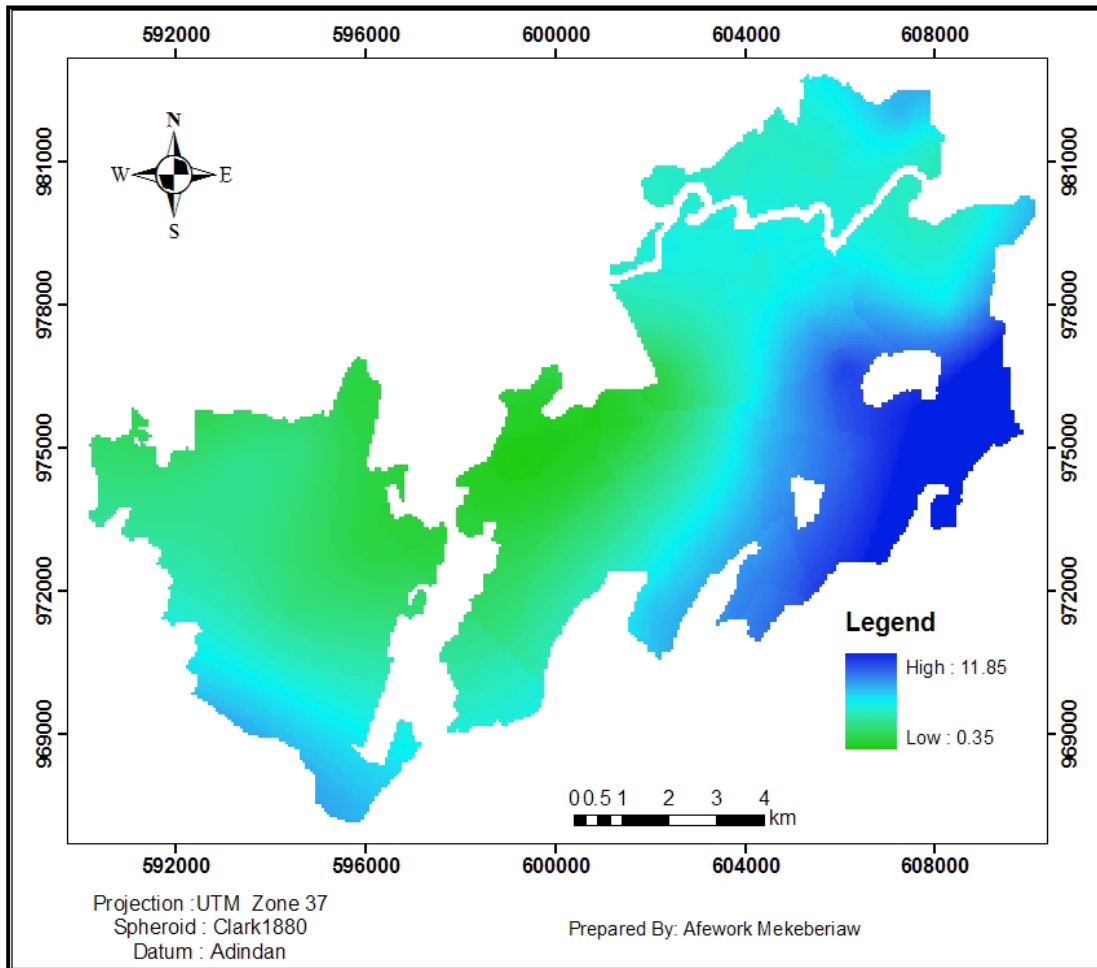


Figure 3.18. Interpolated ground water level of Metehara Sugarcane estate.

After interpolating the point data to areal basis using completely regularized spline interpolation (CRSI), the ground water level map was reclassified with a grid map of 30m-cell size. The reclassified version implies 1 to 3, where 1 stands for the least contributor to salinity and 3 for the class that highly contribute the salinity of the soil (Figure 3.19).

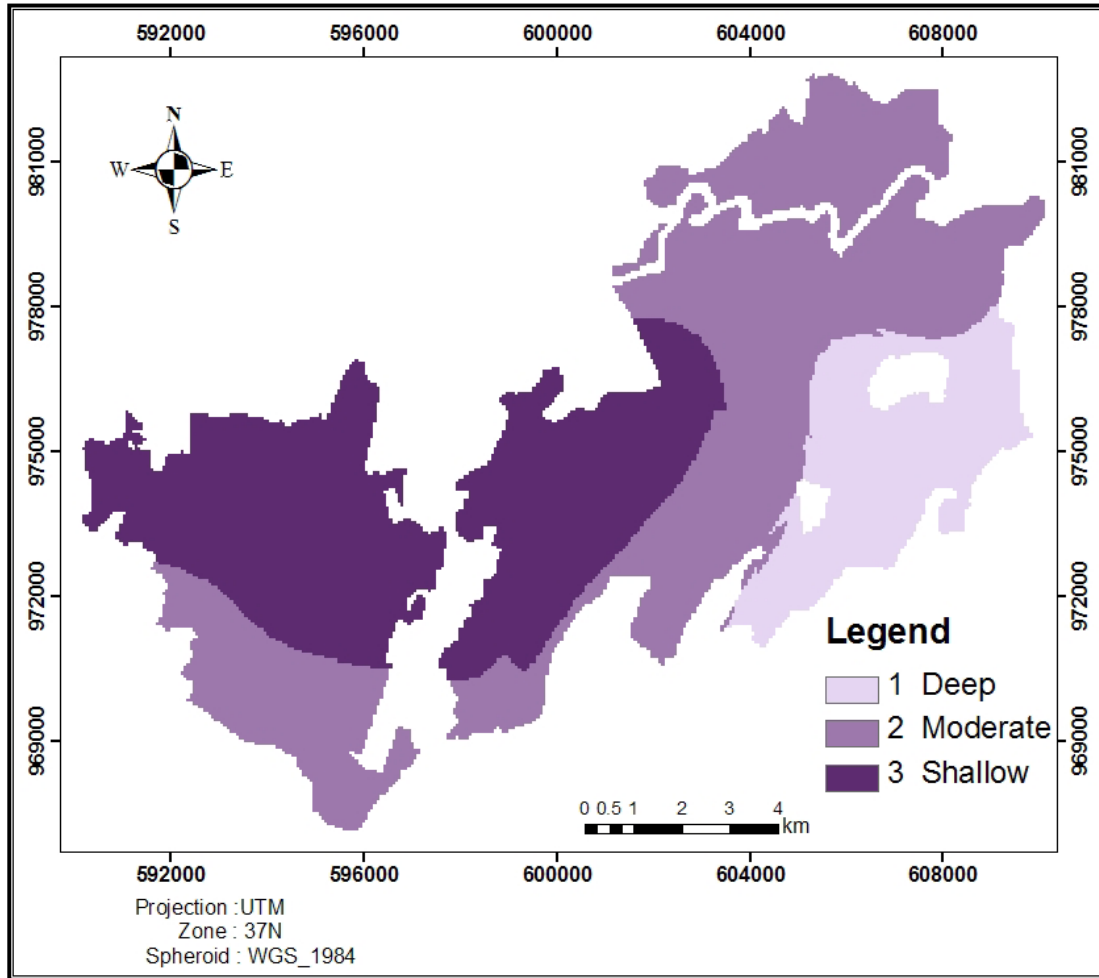


Figure 3.19. Reclassified Interpolated ground water level of Metehara Sugarcane estate.

The Ethiopian rift is characterized by high salinity due to high degree of water-rock interaction, evaporation and the discharge of thermal water. Most waters in the highland volcanics have good to excellent chemical quality, while waters in rift valley are characterized by high Na, HCO<sub>3</sub> and F content (Tamiru Alemayehu, 2006). Therefore, the shallower the ground water depth, is the higher influence to soil salinity model and higher depth of ground water the lower its influence to soil salinity model. As the dissolved ions come to the surface through capillary rise and only H<sub>2</sub>O is evaporated and the dissolved ions remain in the soil.

### 3.3.3 Multi-Criteria Decision Making

In the procedure for Multi-Criteria Evaluation using a weighted linear combination, it was necessary that the weights sum to one. Weights of this nature were derived by taking the principal eigenvector of a square reciprocal matrix of pair-wise comparisons between the criteria (Saaty, 1977). The comparisons were concerned with the relative importance of the two criteria involved in determining salinity vulnerability of the study area.

In developing the weights, every possible pairing was compared and the ratings have been recorded into a pair-wise comparison matrix (Table 3.4). As the matrix is symmetrical, only the lower triangular half was to be filled in. The remaining cells were the reciprocals of the lower triangular half.

Table 3.4. Pair-wise Comparison Matrix

	<b>Ground water level</b>	<b>Geological formation</b>	<b>Land form</b>	<b>Land cover</b>
<b>Ground water level</b>	1			
<b>Geological formation</b>	1/2	1		
<b>Land form</b>	1/3	1/2	1	
<b>Land cover</b>	1/4	1/3	1	1

The principal eigenvector of the pair-wise comparison matrix were computed to produce the best fit set of weights using IDRISI software. Table 3.5 shows the resulting weight for each soil salinity factor. Accordingly, ground water level was weight of 0.46, which shows that it had 46% influence to the salinity of the soil of the study area. Geology, land form and land-cover have had percentage influence of 27 %, 16% and 11%, respectively.

Table 3.5. Factor weights derived by calculating the Principal Eigenvector of the Pair-wise Comparison Matrix.

<b>Factor</b>	<b>Factor weight</b>
Ground water level	0.46
Geological formation	0.27
Land form	0.16
Land cover	0.11

In running the model using weighted overlay analysis, the cell values of each input parameters were multiplied by the computed weight. The resulting cell values are added to produce the final out put raster model. The higher raster values indicate areas that were more saline, whereas lower raster values indicate the areas that were less saline soil.

The output raster, the saline model was reclassified in to four classes ranging from 1 to 4. 1 implies the least saline areas and 4 implies areas with highest salinity problem.

### **3.4 Overlay Analysis of Salt affected soil against different factors**

The spatial distributions of salt affected areas were evaluated based on overlaying with different features. Among the factors considered were canal and drainage layout, soil and piezometric data.

#### **3.4.1 Preparation features for overlaying**

**3.4.1.1 Drainage and Canal Layout:** Both drainage and canal layout were digitized from the map that depict the drainage and canal layout, farm plot partition, piezometric reading location and other features. For the purpose of overlay analysis, the digitized canal and drainage layout were buffered with 100 m distances. Since the problem associated with malfunctioning of canal

and drainage was not confined to only along the line, rather their effects were manifested some distance, both sides, along the canal and drainage line. Therefore, the overlay analysis was done using 100 m buffered drainage and canal layout. Figure 3.20 and 3.21 show the buffered canal and drainage line used in overlay analysis.

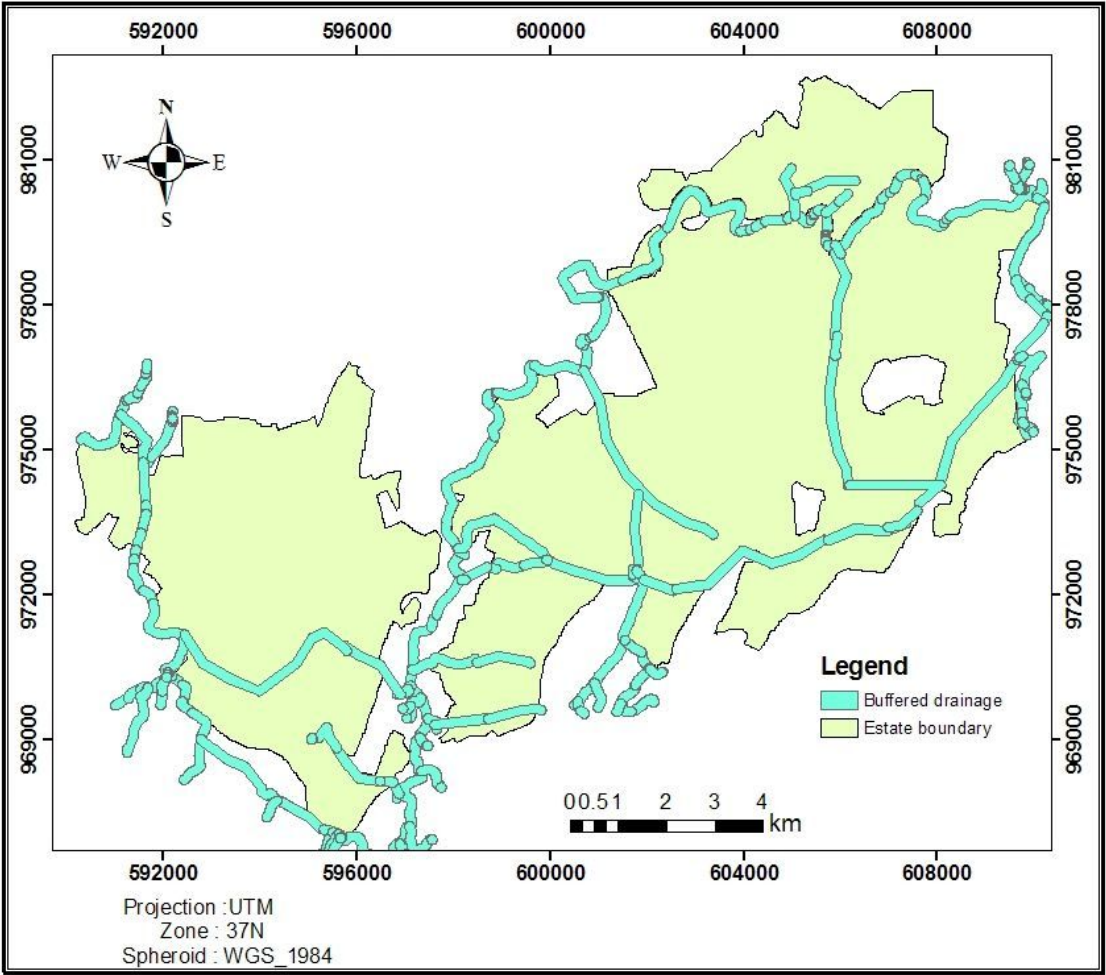


Figure 3.20. Buffered drainage layout of Metehara sugarcane estate.

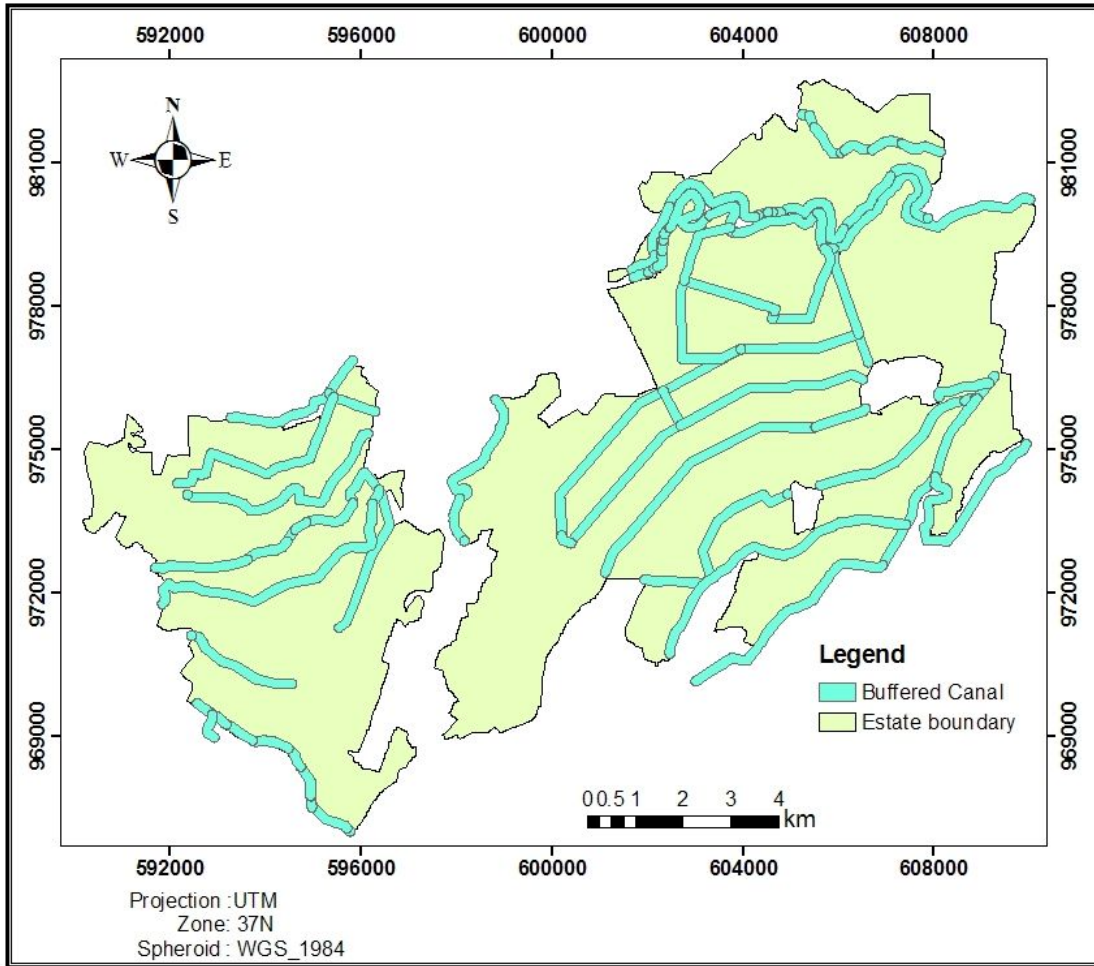


Figure 3.21. Buffered Canal layout of Metehara sugarcane estate.

**3.4.1.2 Piezometric data:** in order to assess the spatial distribution of salt affected area with respect to ground water table, the piezometric data that was collected in the same month as of the image interpreted were used. As soil salinity problem was closely related with shallow water depth, the salt affected areas mapped were overlaid with the ground water table depth. Therefore, the piezometric data was interpolated to generate a continuous surface. For the purpose of interpolation, a total of 37 piezometric data distributed through out the study area were used. Completely regularized spline interpolation (CRSI) was adopted as a method for the purpose of interpolation. Based on the ground water depth, the entire area was classified as critically waterlogged, potentially waterlogged and safe area (Table 3.6 and Figure 3.22).

Table 3.6. Classification of water depth

Depth (m)	Water logging level
0.35 - 2	Critically waterlogged
2 - 3	Potentially water logged
> 3	Safe area

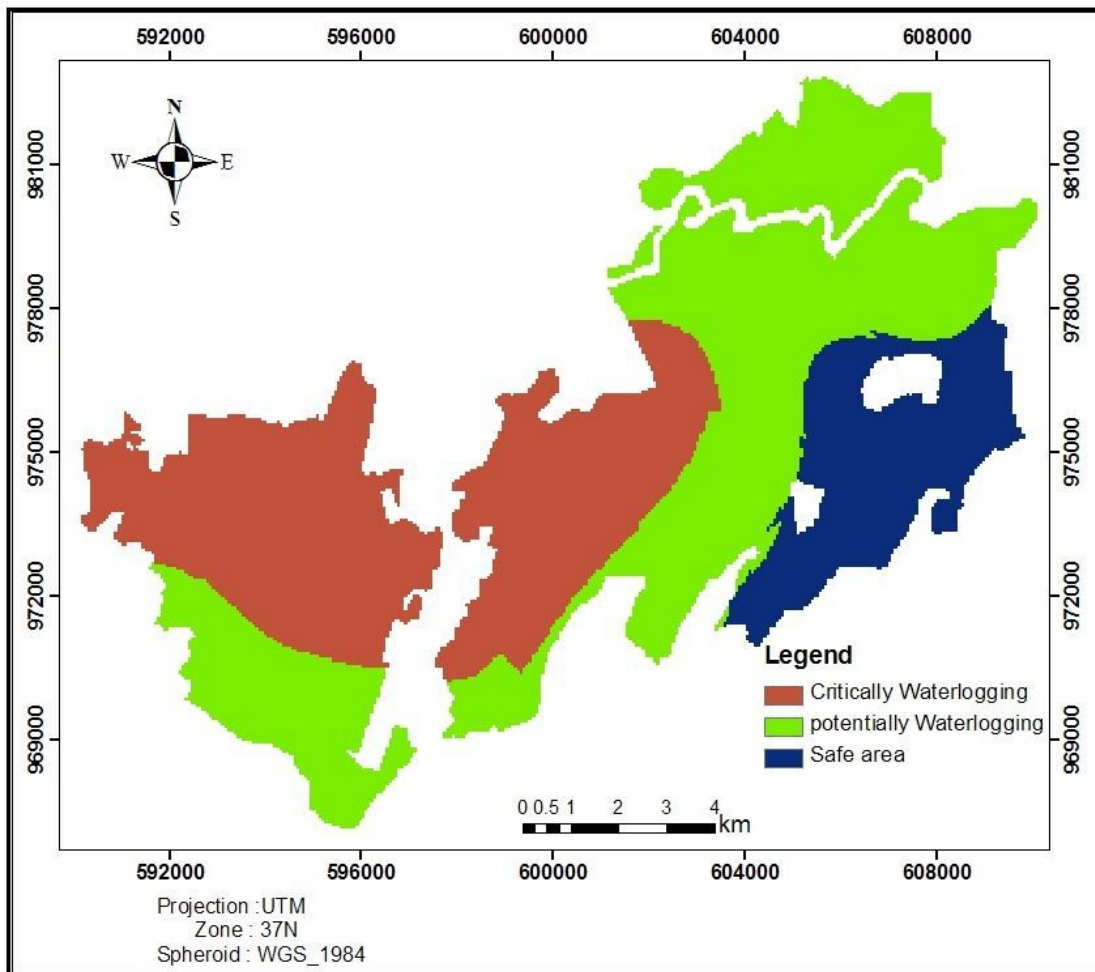


Figure 3.22. Interpolated ground water level classes.

**3.4.1.3 Soil Map:** The soil map used for the overlay analysis (Figure 3.23) has a scale of 1:10,000. The major soil considered were Calcaric Cambisols, Vertic Cambisols, Hypovertic Cambisols, Hypostagnic Cambisols, Hypogleyic Cambisols, Fluvic Cambisols and Eutric Cambisols.

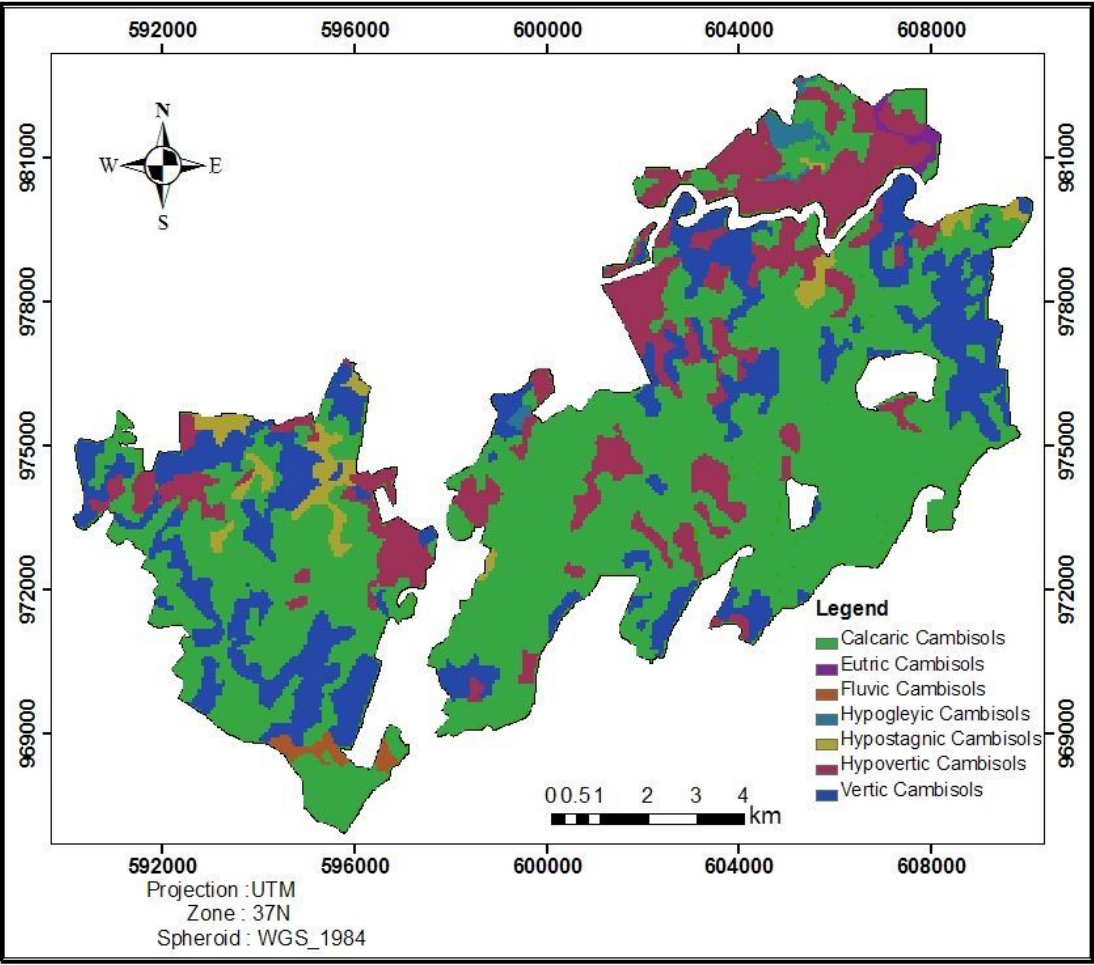


Figure 3.23. Soil map of Metehara Sugarcane estate.

## **4. Results and Discussion**

### **4.1 Distribution of the Salt-affected Areas in the Sugarcane farm**

#### **4.1.1 Salt-affected Areas Characterized by Salinity Levels**

Based on visual interpretation of ETM+ satellite image, coupled with ground truth, the study area are categorized into three salinity levels:

- 1) Severe saline,
- 2) Moderate saline, and
- 3) Slight saline.

The result derived from visual interpretation would not considered as much acceptable. However, it gives a clear idea about the reflectance properties of salt affected area as well as identifying other features.

##### **4.1.1.1 Severe saline**

Severe salinity mostly occurs where the relative reflectance is very high as compared to other features. Different researchers have reviewed that the reflectance of salt affected area is higher in much of the bands other than other features. On the Standard False Colour Composite 4-3-2, the severely salt-affected areas are mostly represented in very bright colour with some small amounts of other colours. The texture of these areas is very fine (See Figure 3.6).

##### **4.1.1.2 Moderate saline**

Moderately salt-affected areas are normally shown in light blue colour on the False Colour Composite. They also show fine texture with few mottled spots of other colours.

##### **4.1.1.3 Slight saline**

Slight salinity is normally shown in pinkish white colour on the False Colour Composite. They normally show a few red or pink mottled textures.

## **4.2 Result from satellite image classification**

### **4.2.1 Results from Supervised Classification**

The results from supervised classification of ETM+ data are shown in Figure 4.1.

These results can be summarized as follows:

As salt affected area, settlement, bare and dry soil have similar reflectance. After field visit, areas which were classified as salt affected before field check were identified and masked out from the overall analysis.

As a matter of fact, soil salinity is a dynamic process that means it changes with time (it differs season to season); the training area given for the supervised classification was based on the knowledge base. The training areas given were based on the reflectance signature and different band combination. As previously mentioned from correlation matrix of bands different band combinations were used (Mainly of 4-3-2, 5-4-3...).

During the field check, some places especially in the central part were still showing salinity effect. Informal discussion and field visit with the experts of Metehara Sugar Factory Research Center was also used as an input for post-classification.

The land-use land-cover map of the Metehara Estate was classified with an overall accuracy of 93.14%. Of the land-use land-cover classes the severely salt affected soil was classified with 96% accuracy but the least accuracy of mapping resulted on water logging classes. The reason behind this is the water logging areas resemble with others land-use land-cover classes and results spectral confusion in classification (see Appendix-III).

The result of final supervised classification shown in Figure 4.1. The land-use land-cover percentage of the estate indicates greater than half part of the area which accounts 67% was covered by well-vegetated and vegetated. There was a significant severely salt affected land about 6% that both dominate southwestern and northeastern part of the estate. From the total area coverage water logging, moderately to slightly salt affected soil and fallow land holds 5%, 12% and 10% respectively (Figure 4.2).

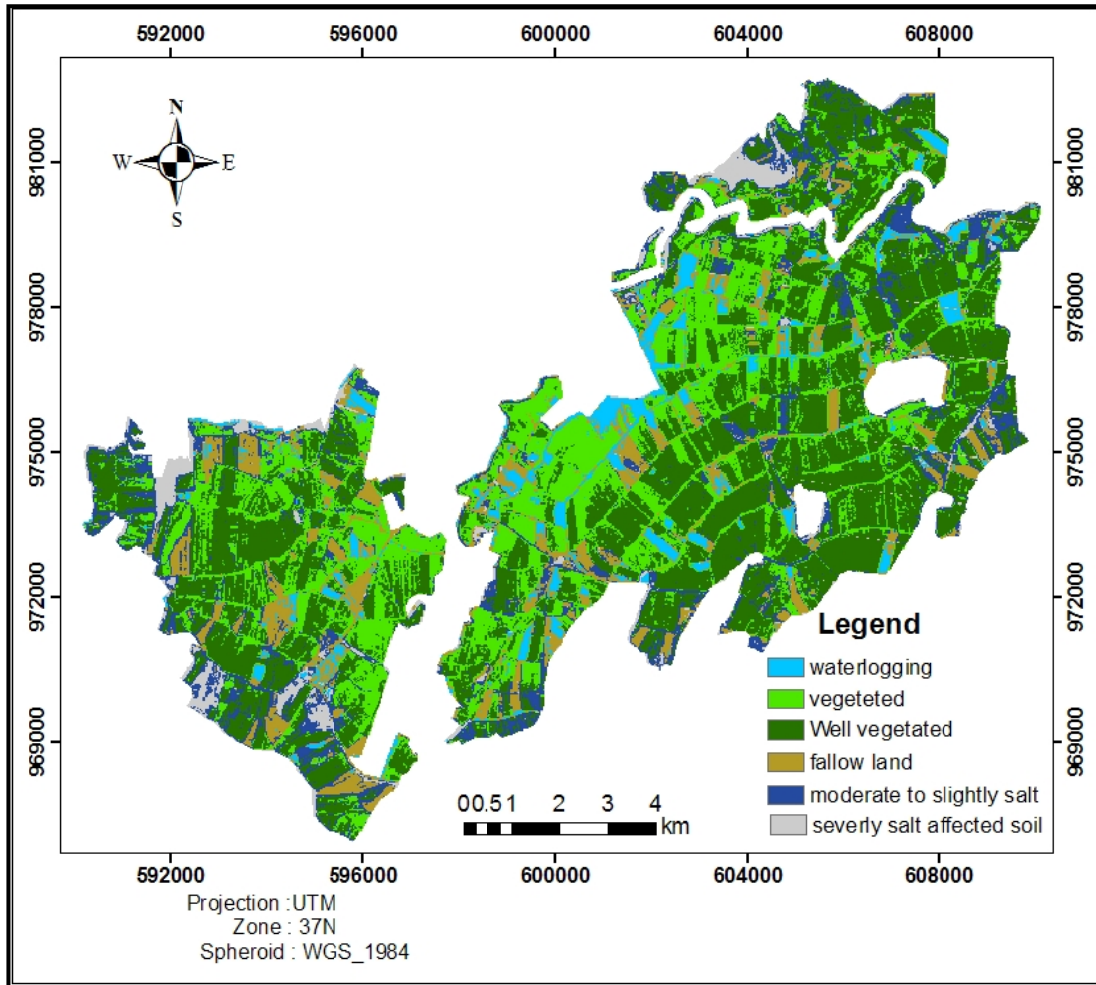


Figure 4.1. Land-use land-cover map.

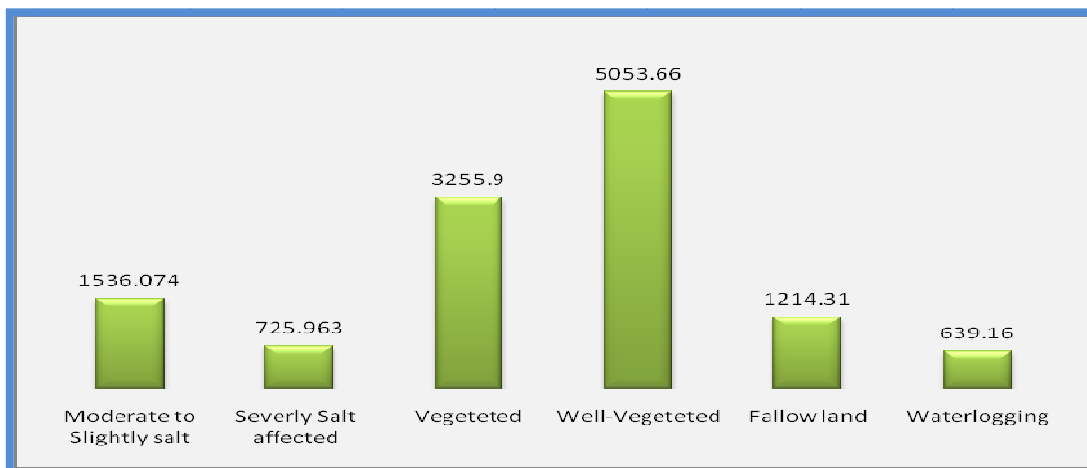


Figure 4.2. Aerial extent of soil salinity derived from land-use land-cover map.

### **4.2.2 Results from Indice Analysis**

From the result of NDSI it was observed that an area with high raster value or high reflectance was delineated as area affected by salinity problem. Once areas having high reflectance value was identified, based on their reflectance value the level of the salinity was determined.

In the NDSI image the salt-affected areas, depicted in gray colour, could be roughly differentiated from those of non-salt-affected areas, water logged (in cyan colour) and vegetation (in green colour). As this salinity problem dynamics in nature even varies with time and the image used was a captured 2005, ground truth only gave slight indications of the presence of salt affected area. However, the extent of the soil salinity problem in the study area was found to be increasing. The salinity level classified in NDSI was given in Figure 4.3. The area-wise distribution is given in the Table 4.1.

Out of the total area, 6% was classified as highly saline which was distributed through out the study area and moderately saline area covers about 20% of the total are. Metehara Sugarcane irrigation farm sites specifically in the Abadir farm around lake Beska, its central and in many part of North Camp farm were found to be highly saline.

As illustrated in Figure 4.3, the central and south-eastern zones of the estate were clearly marked by lower salinity. This region was characterized by undulating topography and far from the influence of Beska lake influence and, hence, well drained. In spite of intensive irrigated sugarcane cultivation, the zone was free from salinity problems.

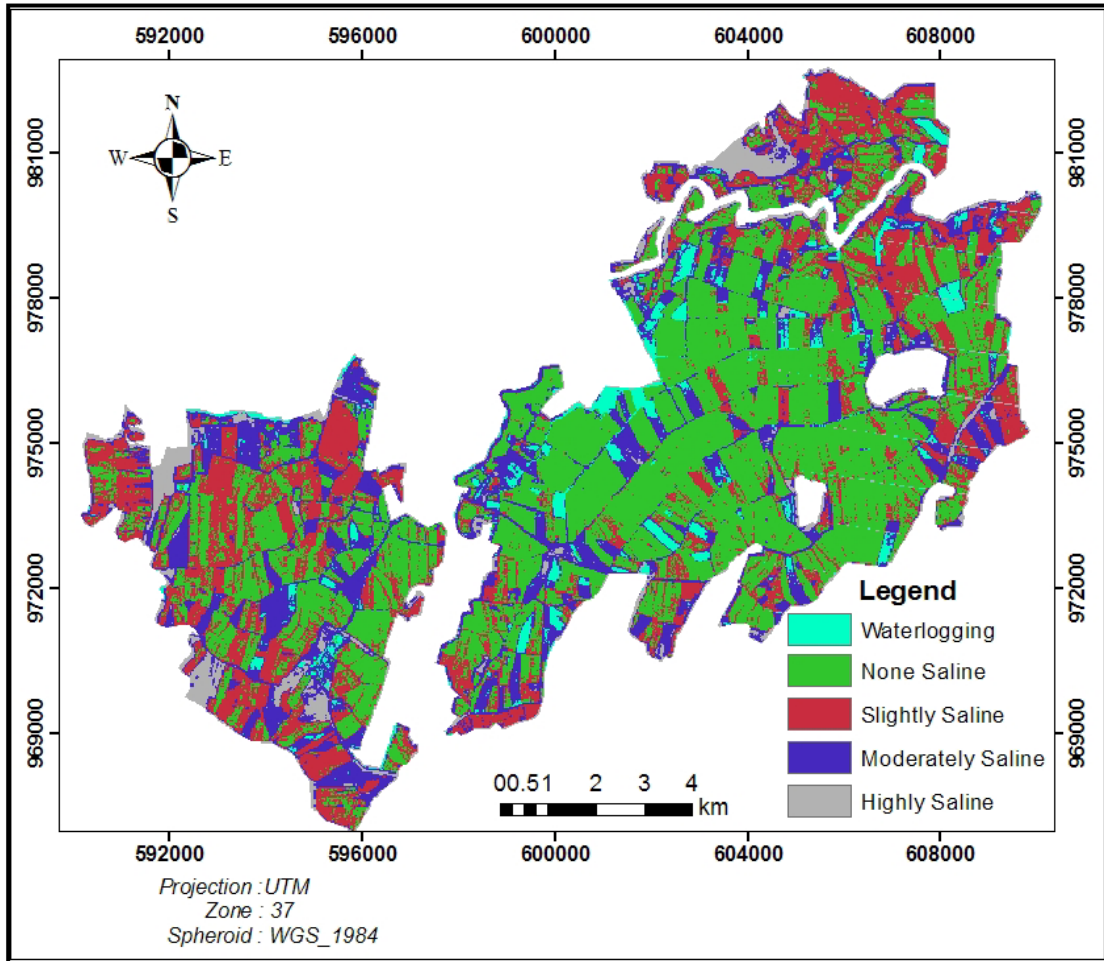


Figure 4.3. Map of Normalized Difference Salinity Index (NDSI).

Table 4.1. Salinity level determined from NDSI in percent.

Class Name	Area (ha)	Area in %
Water logging	490.599	4%
None Saline	5681.53	46%
Slightly Saline	2999.31	24%
Moderately Saline	2474.03	20%
Highly Saline	779.598	6%

### **4.3 Empirical Models Using Soil Salinity (EC)**

Empirical model for E<sub>Ce</sub> vs NDSI was prepared using regression analysis. It was observed that empirical model of E<sub>Ce</sub> vs NDSI offered coefficient of determination 77.5%. This empirical model was extended for the whole image using modeler builder in ArcGIS and salinity levels were divided into three groups. The advantage of this model being generalized through GIS was that it directly gives the salinity level at any point in the image.

This empirical model enhances some new areas of high salinity. From the predicted salinity map three ranges of salinity level was generated. The summary of salinity level, extent of the area in hectare and percentage are given in the Table 4.2 and Figure 4.4.

The empirical model resulted in three salinity classes with varying degree of salinity, namely- highly saline, moderately saline and non saline which cover 7%, 27% and 66% of the total area respectively.

From the output map, one can easily see that those areas categorized as highly saline are located near to lake Beska, North Camp farm, central part of Abadir farm and flat slope areas of the estate. Hence, such spot areas are highly concentrated and located in the northern and south west parts of the study area with total area coverage of 838.7 ha of land. These areas are represented/ shaded with rose colour in the salinity map.

Finally, the spatial distribution of salt affected land derived from empirical model were checked by comparing it with salt affected area derived from NDSI and indicates that the same areal extent in highly saline class but other classes did not show significant relation.

Table 4.2. Salinity level and extent derived from empirical model.

Item	Salinity level (dS/m)	Salinity Extent	Area(ha)	Area in %
1	0.75-4	Non saline	8202.91	66
2	4-8	Moderately saline	3383.43	27
3	>8	Highly saline	838.729	7

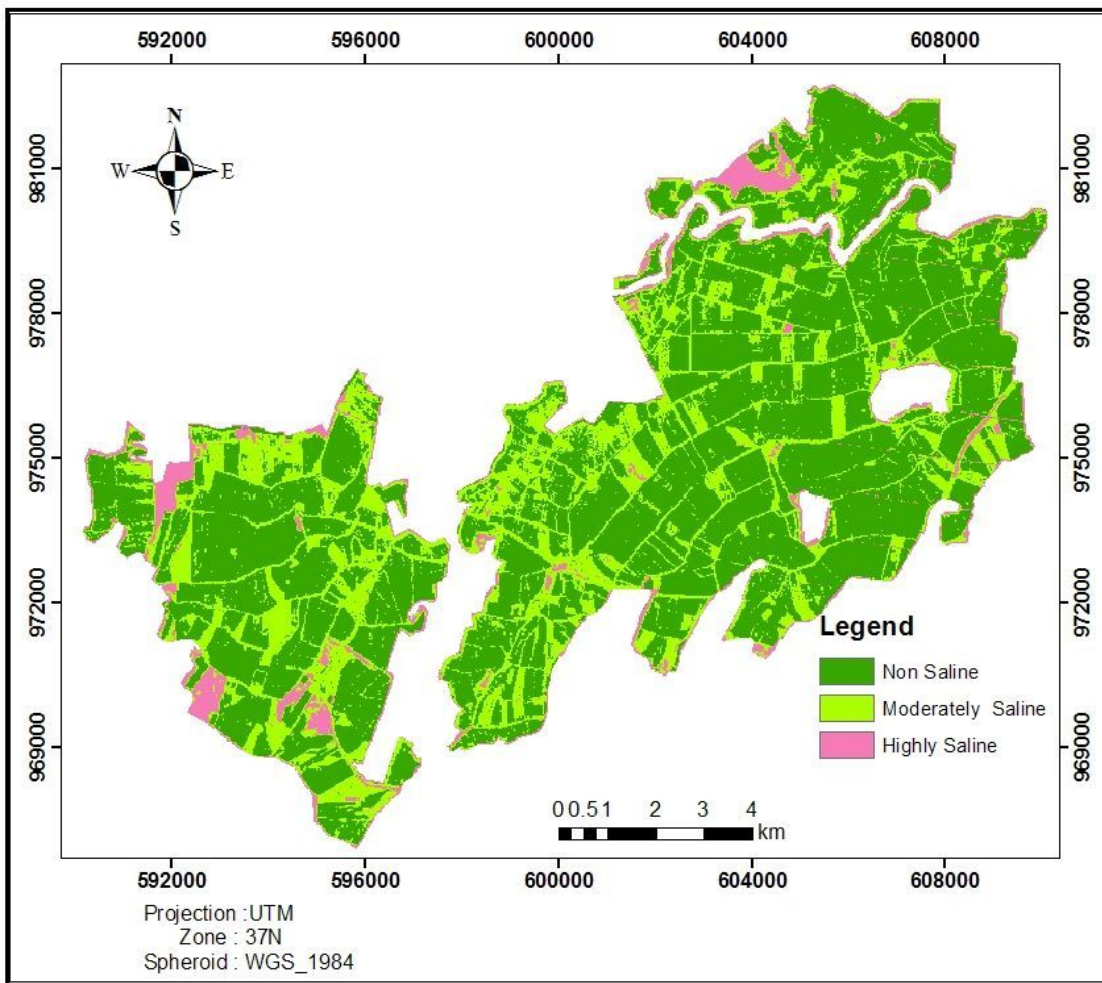


Figure 4.4. Salinity map generated from empirical model.

## 4.4 Result from Overlay Soil Salinity Model

### 4.4.1 Salinity Model

The model of salinization in the Metehara Sugarcane estate irrigation farm consists of four factor layers:

$$\text{Salinity} = (0.46 \times \text{ground water level}) + (0.27 \times \text{Geology}) + (0.16 \times \text{Landform}) + (0.11 \times \text{Land cover})$$

According to the salinity model result, four classes were identified with varying degree of salinity (Figure 4.5 and 4.6). The highly saline soils were found on the areas underlain by the lacustrine sediments and shallow ground water level. The low lying topography and poor vegetation cover greatly enhanced the salinization. The extent areas of each class of the salinity are shown in Table 4.3. The high and moderate soil salinity classes cover approximately 11 % and 40 % of the total area, respectively. The non and slightly saline soil classes together accounted for over 49% of the total area. It is evident that the areas highly vulnerable to salinization greatly related to the ground water level that normally occurred on the lacustrine sediment near to lake Beseka.

Table 4.3. Extent of areas of various salinity levels derived from overly salinity model.

Item	Salinity Extent	Area(ha)	Area in %
1	Non Saline	2816.957	23
2	Slightly Saline	3229.28	26
3	Moderately Saline	4999.84	40
4	Highly Saline	1378.99	11

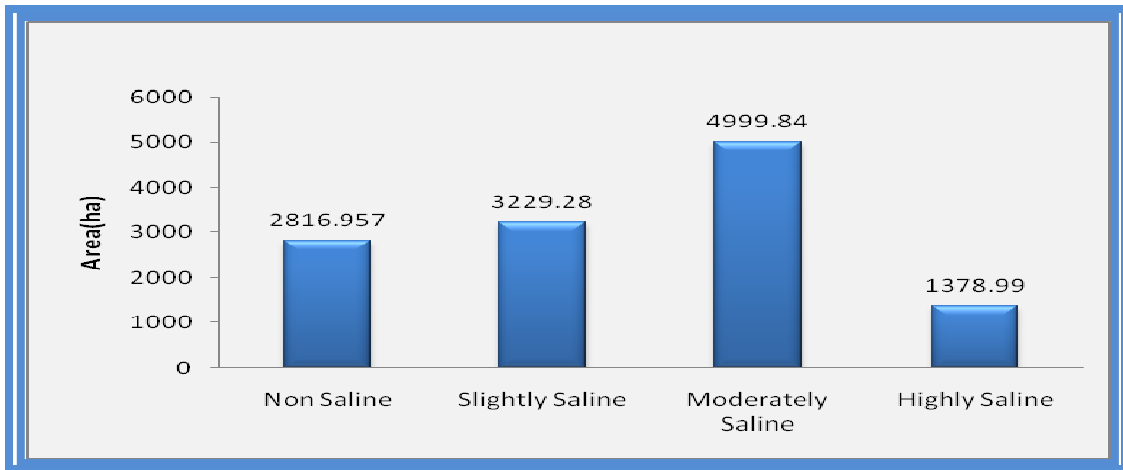


Figure 4.5. Salinity level derived from overlay salinity model.

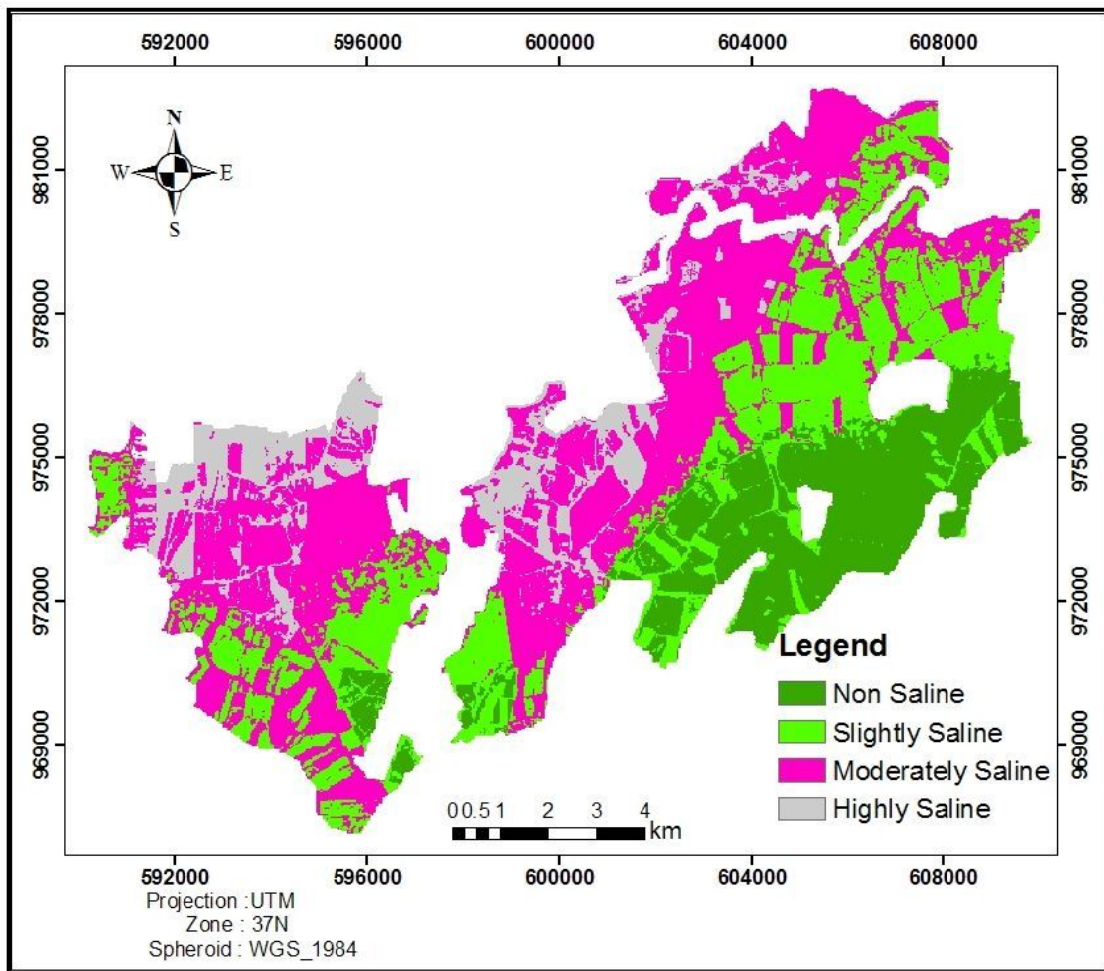


Figure 4.6. Salinity map of Metehara sugarcane estate generated from overlay salinity model.

## 4.5 Validation and Comparison of the Methods

The EC value with the corresponding raster value of the salinity map generated by satellite imagery and overlay salinity model developed from four thematic layer plotted on a scatter diagram and the validation of the model were carried out by the existing EC value with referenced to the same locations.

Figures 4.7 and 4.8 show that in empirical model the correlation between ECe and NDSI has less correlation where as in the overlay salinity model, the correlation between ECe and the raster value of the model do have higher correlation (66%) than empirical model. Therefore, the overlay salinity model can be used to predict soil salinity in the study area more accurately than empirical model.

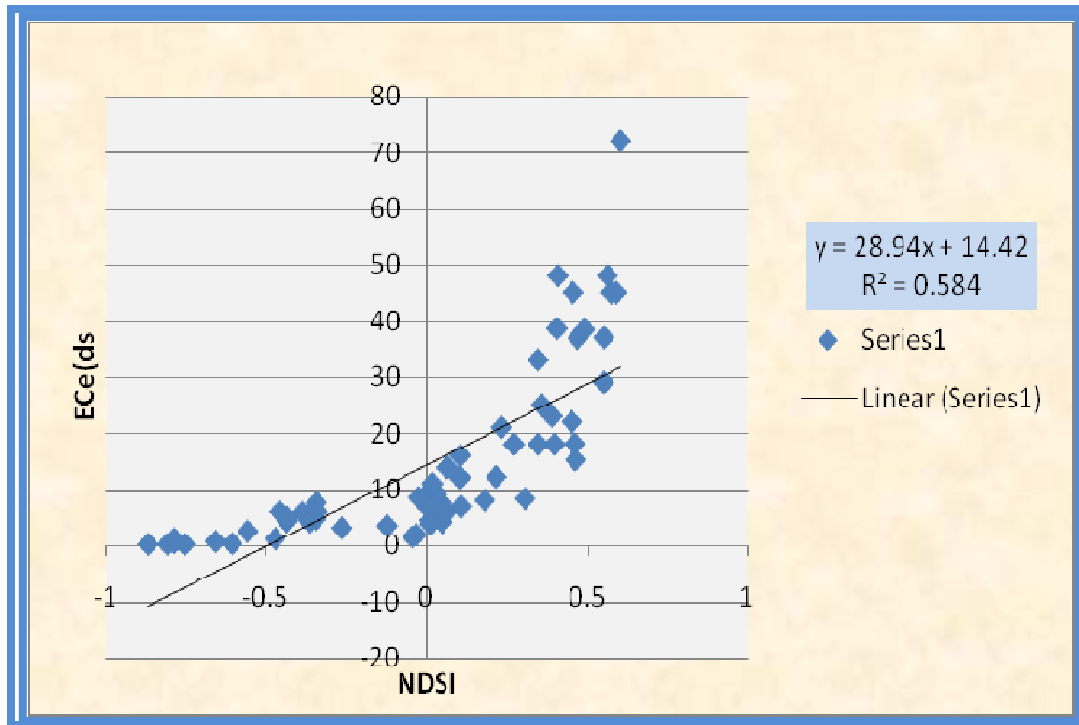


Figure 4.7. Correlation of ECe and raster value of NDSI.

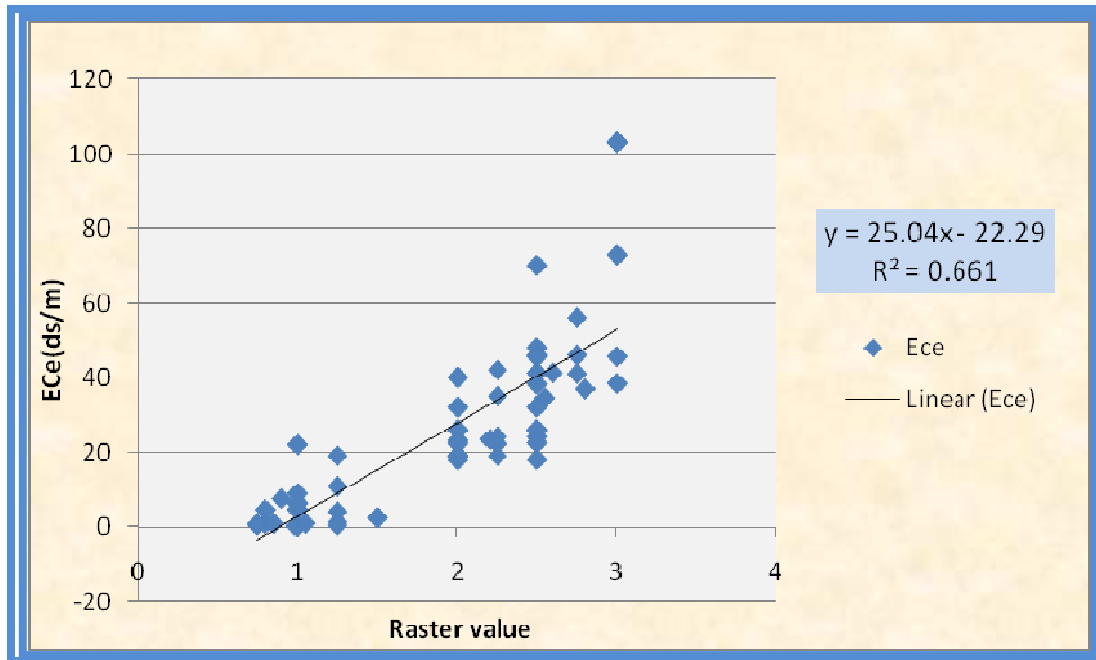


Figure 4.8. Correlation of Ece and raster value of overlay salinity model.

## 4.6 Results from Overlay Analysis of Salt-affected Soil against the Different Factors

After salt affected areas were identified, attempts were made to assess their spatial distribution in relation to the following:

- Canal
- Drainage
- Water table
- Soil

### 4.6.1 Canal vs Map of salt affected soil generated from Overlay soil salinity model

The total area identified as salt affected soil was 1379 ha out of this 20.3 % (279.9ha) was lying within 100 m from the canal line (Figure 4.9). According to Maher and EL-Sayed (2000), poor irrigation water management system leads to secondary salinization. Secondary salinity, resulting from modern irrigation occurs because of accelerated redistribution of salts in the profile by high water tables or use of insufficient water to leach salts out of the soil.

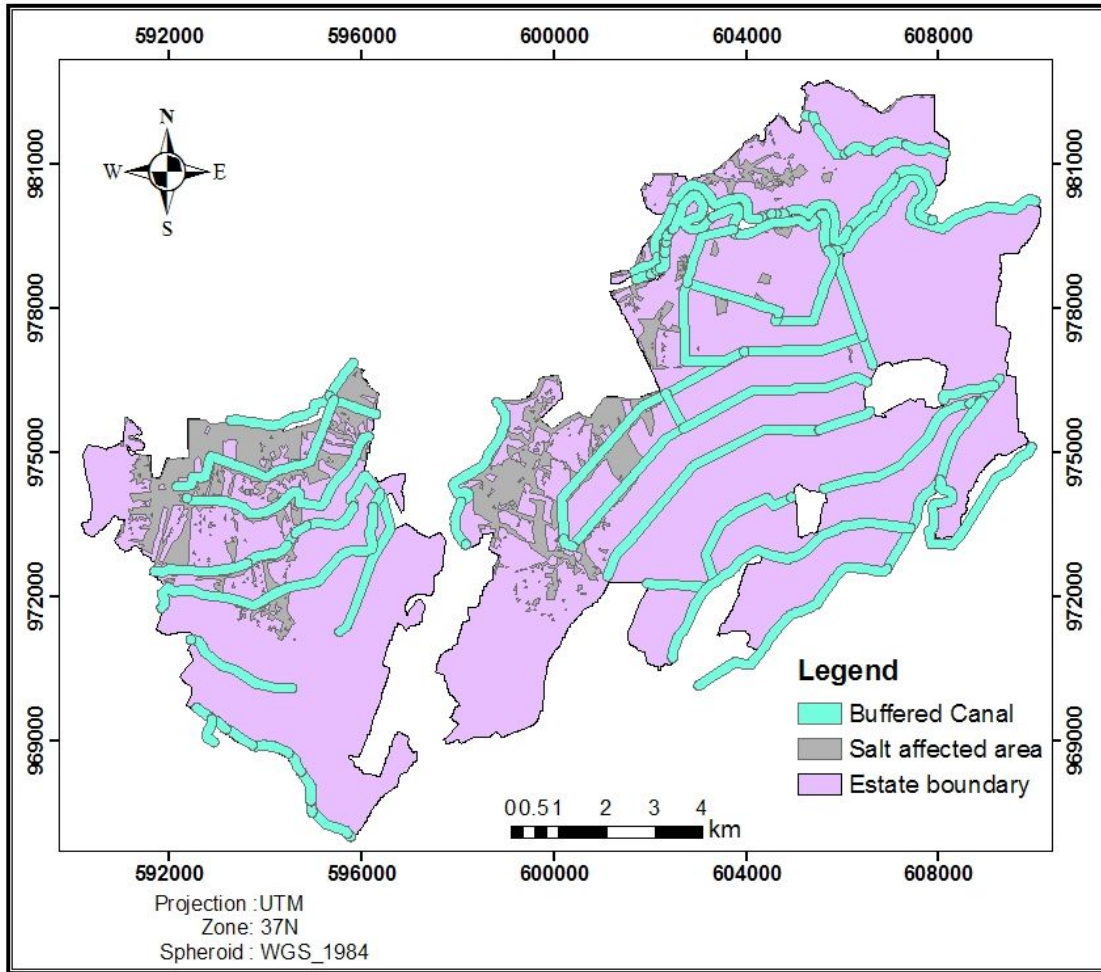


Figure 4.9. Salt affected area vs canal.

#### 4.6.2 Drainage vs Map of salt affected soil generated from Overlay salinity model

The area of salt affected soils that resides within 100m distance of drainage is found (Figure 4.10) to be only 5.4% (74.43ha). This result indicates the contribution of the surface drainage in eliminating excess water relatively good. Since, in many areas drainage problems arise because of the accumulation and stagnation of excess irrigation water on the soil surface.

Surface drainage problems usually arise due to slopes that are too flat or to slow water penetration because of structural instability of the soils or to uneven land (Girume Bekele, 2005). Therefore the surface drainage of the study area can be evaluated as good since the problem of soil salinity around drainage area is low.

However, salt affected areas that are away from drainage line salt accumulation may be due to poor drainage system. But, further investigation is needed to see their relationships.

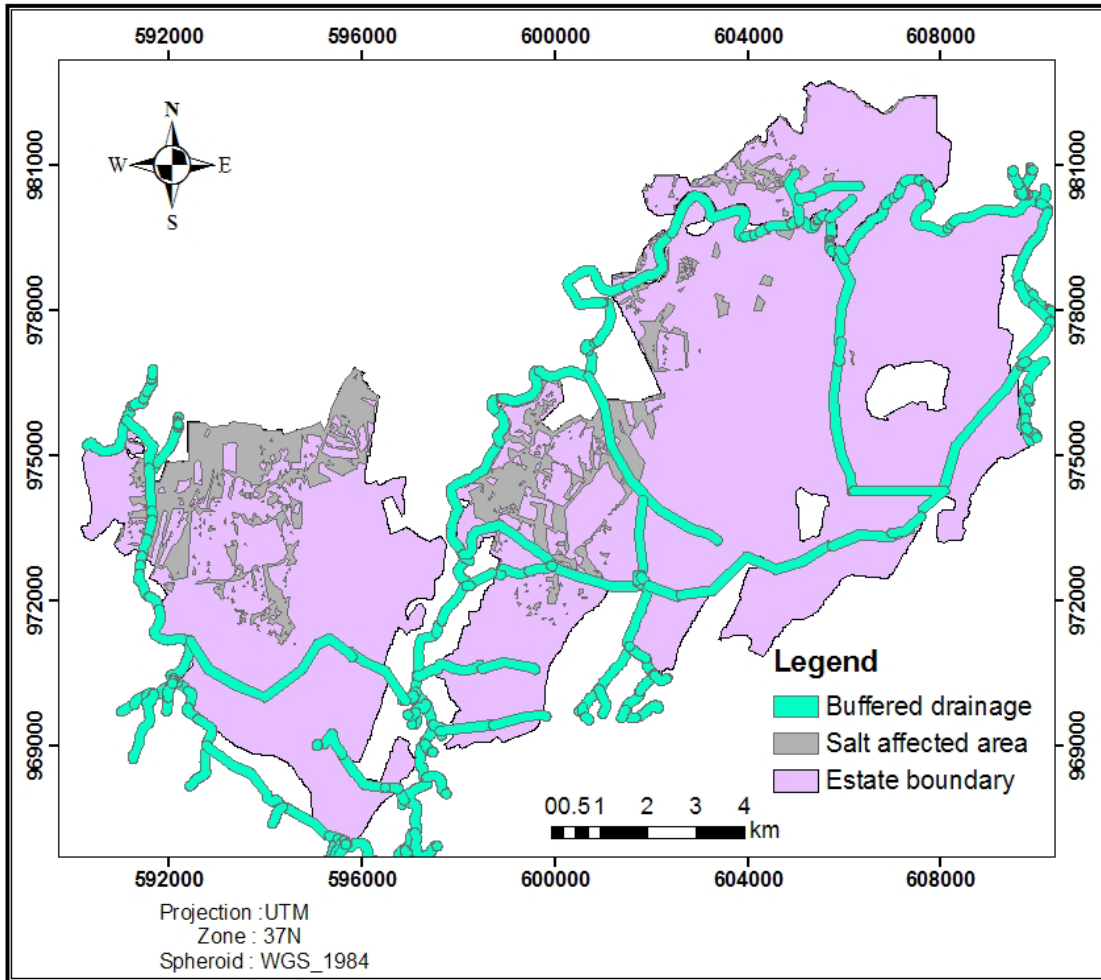


Figure 4.10. Salt affected area vs surface drainage lines.

#### 4.6.3 Soil vs Map of salt affected soil generated from Overlay salinity model

In the study area there are seven major soil types: Calcaric Cambisols (57% of the total area), Vertic Cambisols (19% of the total area), Hypovertic Cambisols (17% of the total area), Hypostagnic Cambisols (3% of the total area), Hypogleyic Cambisols (1.6% of the total area), Flulvic Cambisols (1.4% of the total area) and Eutric Cambisols (1% of the total area).

From the overlay analysis, out of the total of 1379ha of salt affected area, 41.6% resides on Calcaric Cambisols which by far occupies the major area (Figure 4.11), 23.2 % is on Vertic

Cambisol, 25.2% on Hypovertic Cambisols, and the rest 10% of salt affected area found on Hypostagnic Cambisols, Hypogleyic Cambisols and Eutric Cambisols .This result indicates the relative distribution of salt affected area is not significantly affected by soil type, as all type of soils are comparably affected according to their aerial extent.

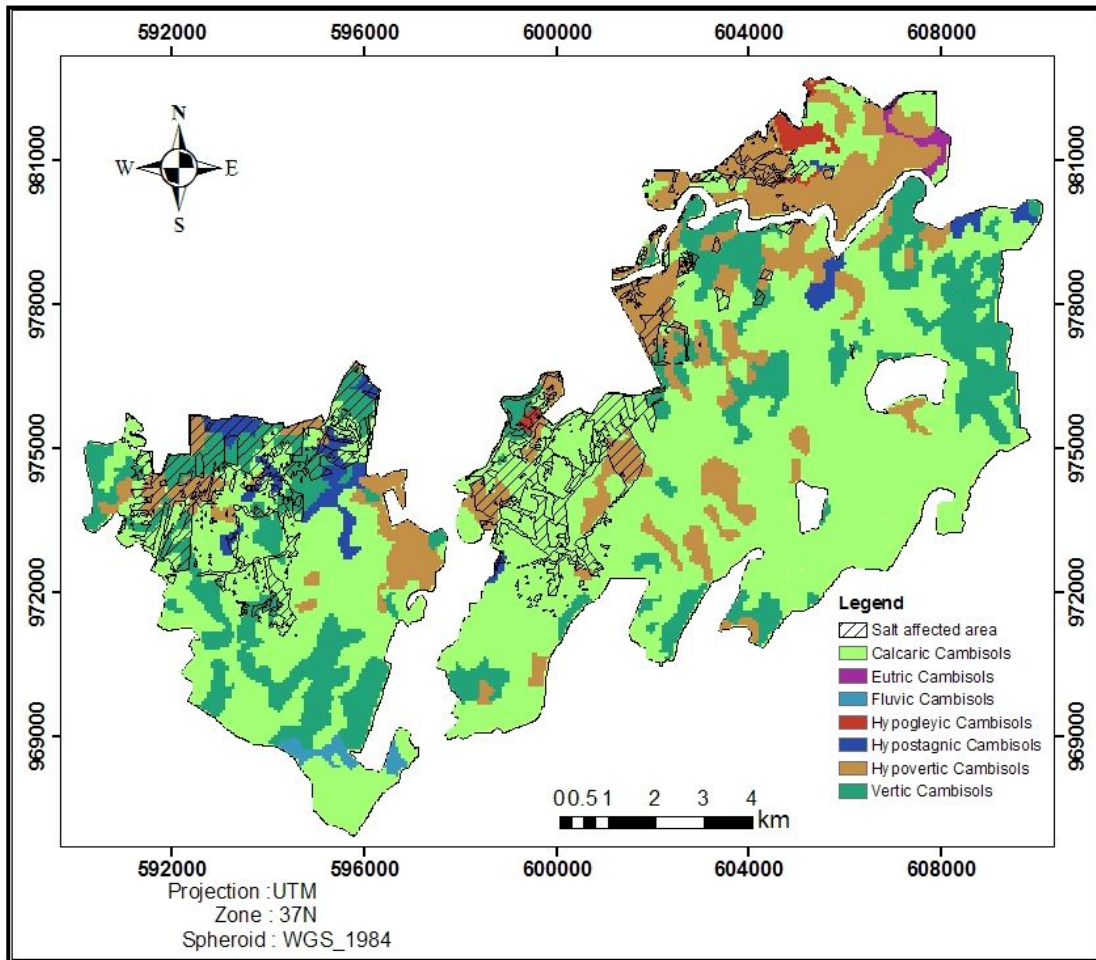


Figure 4.11. Salt affected areas vs major soil types of the study area.

#### 4.6.4 Water Table vs Map of salt affected soil generated from Overlay salinity model

The spatial distribution of salt affected area has been assessed based on the classification of water table depth (See Table 3.6). From the overlay analysis the result is summarized in Figure 4.12. The total area being identified as salt affected soil is 1379 ha, out of this 88 % (1213.5 ha) is lying within critically water logging and 11% is lying in potentially water logging class, but in safe area only 1% of the total salt affected soil exists (Figure 4.13)

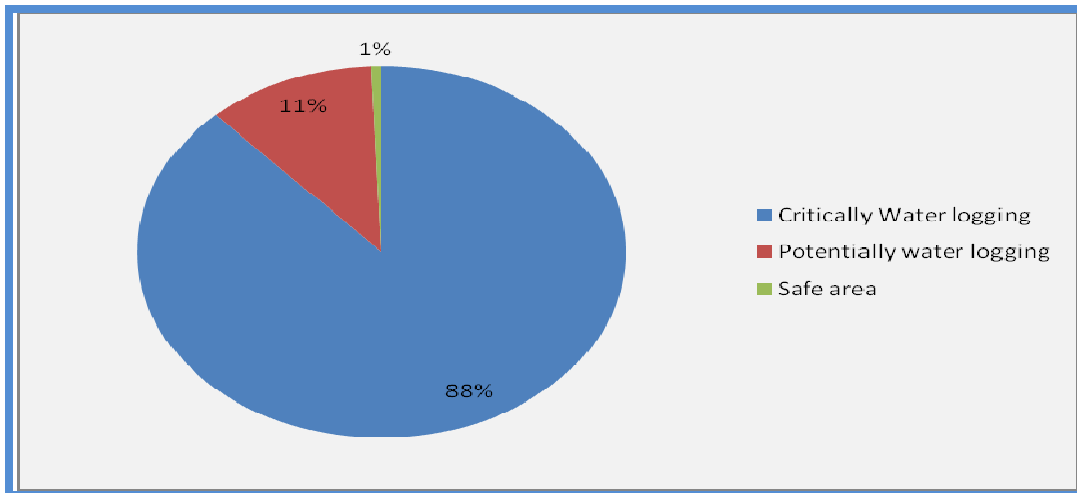


Figure 4.12. Spatial Distribution of salt affected soil vs water table depth.

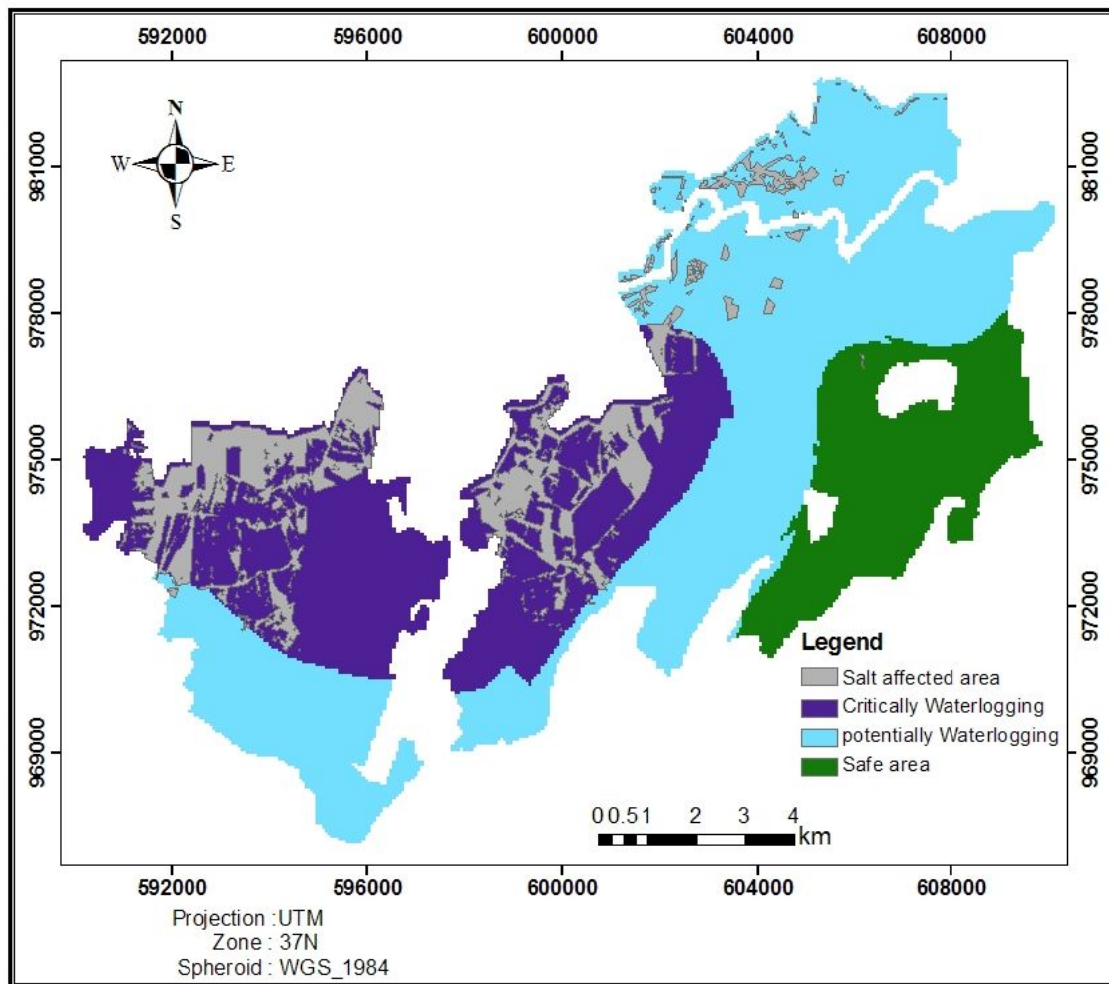


Figure 4.13. Salt affected areas vs water table depth.

## **5. Conclusions and Recommendations**

### **5.1 Conclusions**

This study showed that the visual interpretation, unsupervised and supervised classifications were good indication of soil salinity. However, the result obtained from these methods vary in aerial extent, the spatial location being determined as salt affected areas are similar. Therefore, visual interpretation and image classification are found to be important in salinity mapping.

The Normalized Difference Salinity Index (NDSI) has shown that from the total area only 6% is highly salt affected. This shows not only the extent of salt affected area but also the level of salinity based on their reflectance value. NDSI can be used for the demarcation of salinity affected area depending on salinity incrustation on soil surface and stress in vegetation. However, the application of the NDSI is found to be good indication of the presence of soil salinity in the study area.

Empirical model was done for EC values and the corresponding spectral value of the NDSI image. It was found that EC comparatively related to the reflectance patterns on the NDSI images, i.e. in most of the cases the areas with the highest reflectance that appear as brightest on the NDSI images do have the highest EC. Since EC is variable in the field, the relation was fitted into second order polynomial with  $R^2$  of 77%. Using the regression model derived salinity map was generated and the maximum and minimum EC values predicted were 29 and 0.75dS/m, respectively. This empirical model supported with less ground data but representing entire area could give good result especially assessing the salt crust areas.

The overlay salinity model method that indicates the presence of soil salinity in the higher raster values, specifically in areas identified as higher electrical conductivity (EC) by laboratory analysis methods. Therefore the application of overlay salinity model is a good indicator of the presence of soil salinity and it can be used as one of the main inputs for soil management. It may influence decisions of reclamations of soil salinity.

From the validation and comparing the model result, it can be concluded that, the overlay salinity model is found to be a better indicator of soil salinity than empirical model. The reason that empirical model method gives less correlation is that detects only the salts on the surface of the soil and gives a poor idea about the conditions below the surface, while the overlay salinity model method indicates the condition and existence of salt in the entire soil section between the surface and root zone.

However, the correlation between empirical model and soil salinity is less than the overlay salinity model's correlation coefficient; it could be an efficient parameter for preparing soil salinity maps from remotely sensed data. The results presented in this thesis show the feasibility of using remote sensing and GIS data to estimate soil salinity. Compared to the labour, time, and money invested in field work devoted in collecting soil salinity data, the availability and ease of acquiring satellite imagery and other ancillary data are very attractive and efficient.

The result from overlay analysis between salt affected areas and canal, drainage and soil type, did not show significant relation. But, the ground water level does have significant relation with soil salinity and influence the spatial distribution of salt affected soil in the study area.

## **5.2 Recommendation**

From the overall work and results obtained the following recommendations are suggested.

- Despite the fact that the overlay salinity method is simple and easy to apply, the entire relationship changes with time and location. Therefore, this requires frequent field visits to adjust the parameters being considered (both field salinity level as well as the model parameters).
- The empirical method detects only the salts on the surface of the soil and gives a poor idea about the conditions below the surface; so subsurface information should be obtained indirectly with overlay salinity methods. Since the overlay salinity method applied in this study reveals the presence of soil salinity with its extent.

- Using Landsat ETM+ image, it is possible to map salt affected areas. The spatial resolution of satellite images still limits to detect small patches of salt affected area. Therefore, high-resolution images should be applied to map small areas.
- In order to assess reliability of the method applied, it is recommended to execute similar studies in the rift valley having similar agro-ecological conditions.
- Soil salinity processes are highly dynamic. Therefore, the method of detecting soil salinity should also be dynamic.
- Additional research is needed to refine the methodology and determine what tools and technologies are best suited to improve the accuracy of remote sensing and GIS to map soil salinity.

## References

- Ashley, R. P. and Burley, M. J. (1994). Controls on the occurrence of fluoride in groundwater in the Rift Valley of Ethiopia. **In:** *Groundwater Quality*, pp. 45-54, Chapman and Hall, New York.
- Baber, J.J. (1982). Detection of crop conditions with low-altitude aerial photography. **In:** *Remote Sensing for Resource Management*, pp. 407-412, C.J. Johannsen and J.L. Sanders, Iowa.
- Berhanu Gizaw (1996). The origin of high bicarbonate and fluoride in waters of the Main Ethiopian Rift Valley, East African Rift system, *Journal of African Earth Sciences*, **22**:391-402.
- Booker, T. (2005). Feasibility Study of Land Development for Sugarcane Plantation at Metehara Sugar Factory. Masters Court, Oxfordshire.
- Booker, T. (2008). Re-evaluation of plantation soils at Metehara Sugar Factory. Draft Final Report .Masters Court, Oxfordshire.
- Carver, S.J. (1991). Integrating Multi-Criteria Evaluation with Geographical Information Systems. *International Journal of Geographical Information Systems*. **5**:321-329.
- Darling, W. G., Gizaw, B. and Arusei, M. K. (1996). Lake-groundwater relationships and fluid-rock interaction in the East African Rift Valley: Isotopic Evidence. *Journal of African Earth Sciences*. **22**:423-428.
- Dwivedi, R.S. (1996). Monitoring of salt affected soils of the Indo-Gangetic alluvial plains using principal component analysis. *International Journal of Remote Sensing*. **17**:1907-1914.
- Fantahun Abegaz (2007). Report on Salinity problem in Ethiopia. *Third International Workshop on water management Project*, Haromaya University, Haromaya.
- FAO (1976). *A Framework for Land Evaluation*, Soils Bulletin 32. Food and Agricultural Organization, Rome.
- Girume Bekele (2005). The Nature and properties of salt affected soils in middle Awash Valley of Ethiopia. *Journal of Soil Science*, **8**:23-30.
- Goosens, R., Joshi, D.C and Ranst, E.V. (1998). The use of remote sensing to map gypsiferous soils in the Ismailia soil (Egypt). *Geoderma*, **87**:47-56.

- Halcrow (1989). *Master Plan for the Development of Surface Water Resources in Ten Awash Basin*, Vol.6. Ministry of Water Resources, Addis Ababa.
- Heidweiller, V. (1990). Fluoride removal methods. **In:** *Proceedings of the Symposium on Endemic Fluorosis in Developing Countries: Causes, Effects and Possible Solutions*. NIPG-TNO, Leiden. pp. 518.
- [http://www.cadcorp.com/products\\_geographical\\_information\\_systems/saltmod\\_gis.htm](http://www.cadcorp.com/products_geographical_information_systems/saltmod_gis.htm) accessed on 12.03.2009.
- [http://www.esri.com/librarybrochures/pdfs/gis-for-salt affected soil.pdf](http://www.esri.com/librarybrochures/pdfs/gis-for-salt%20affected%20soil.pdf) accessed on 14.03.2006.
- Lillesand, T. M. and Kiefer, R. W. (1994). *Remote Sensing and Image Interpretation* (3rd ed.). John Wiley & Sons, Inc., New York.
- Indo-Dutch Network Project (IDNP) (2002). *A Methodology for Identification of Waterlogging and Soil Salinity Conditions Using Remote Sensing*. CSSRI, Kamal and Alterra-ILRI, Wageningen. pp.78.
- Johnston, R. M. and Barson, M.M. (1993). Remote-sensing of Australian wetlands. An evaluation of landsat TM data for inventory and classification. *Australian Journal of Marine and Freshwater Research*. **44**:235–242.
- Kalra, N.K. and Joshi, D.C. (1997). Evaluation of multi-sensor data for delineating salt-affected soils in arid-Rajasthan. *Journal of the Indian Society of Remote Sensing*. **25**:79-91.
- Kauth, R.Y. and Thomas, G.S. (1976). The tasseled cap-A Graphic Description of the spectral-Temporal Development of Agricultural Crops as seen by Landsat. **In:** *proceeding of the symposium on Machine processing of Remotely Sensed Data*. Purdue University of West Lafayette, Indiana, pp. 41-49.
- Maher, N. N. and EL-Sayed, E.H. (2000). Effects of irrigation water salinity and leaching fraction on the growth of six halophyte species, *Journal of Agricultural Science*. **135**: 279-285.
- Metternicht, G. and Zink, J.A. (1996). Spatial discrimination of salt and sodium affected soil surfaces. *International Journal of Remote Sensing*. **18**:2571-2576.
- Matternicht, G. and Zinck, J.A. (2003). Remote sensing of soil salinity: potentials and constraints. *Remote sensing of Environment*, **58**:1-10.
- Mekamu Kedir (2007). Spatial Discrimination and mapping of soil salinity using Remote Sensing and GIS techniques in the middle Awash basin. Unpublished MSc Thesis, Addis Ababa University, Addis Ababa.

- Metahara Sugar Factory (2006). Assessment of Sugarcane Production Constraints at Metahara: Annex 1, Specific Field Problems.
- Meyer, M.P. (1995). Place of small-Format Aerial Photography in Resource surveys. *Journal of Forestry*, **80**:15-17.
- Ministry of Water Resources, (MoWR) (1999). Database Compilation and Analysis Project. Preliminary Report. Ernst & Young, Dublin.
- Mohr, P. (1971). Ethiopian Rift and Plateaus: Some Volcanic Petrochemical Differences. *Journal of Geophysical Research*, **76**:1967-1974.
- Mongkolsawat, C. and Thirangoon, P. (1990). A Practical Application of Remote Sensing and GIS for Soil Salinity Potential Mapping in Korat Basin, Northeast Thailand. Khon Kaen University.
- Moulders, M.A. (1987). Remote sensing in soil science. **In**: *Developments in Soil Science*. Elsevier Publication, Amsterdam.
- MWR (1999). Study of lake Beseka. Main Report (volume 1). Ministry of Water Resources. Addis Ababa. pp. 200-203.
- Nasir, M. K., Dhinwa, P.S. and Yohei, S. (2001). Land degradation due to hydro-salinity in semiarid regions using GIS and Remote sensing, Department of Biology and Environmental Engineering, Graduate School of Agricultural and Life Sciences, The University of Tokyo 1-1-1 Yayoi, Bunkyo-ku, Tokyo.
- OWWDSA (2007). Soil Survey and land Evaluation Report. Fentale Irrigation Based Development Project, Unpublished Feasibility Study. Oromia Water Works Design and Supervision Authority. Addis Ababa.
- Rao, B. R. and Venkataraman, L. (1991). Mapping the magnitude of sodicity in part of the Indo-Gangetic plains of Uttar Pradesh, northern India using Landsat data, *International Journal of Remote Sensing*. **12**:419-425.
- Rao, M., Sastry, S.V.C., Yadav, P.D., Kharod, K., Pathan, S.K., Dhinwa, P.S., Majumdar, K.L., Sampat Kumar, D., Patkar, V.N. and Phatak, V.K. (1997). A Weighted Index Model for Urban Suitability Assessment-A GIS Approach. Bombay Metropolitan Regional Development Authority, Bombay.
- Richards, L. A. (1954). Diagnosis and improvement of Saline and Alkali soils, Handbook no. 60, USDA.
- Richardson, A.J., Gerbermann, A.H., Gausmann, H.W. and Cuellar, J.A. (1976). Detection of saline soils with skylab multi-spectral scanner data. Photogrammetric Engineering and Remote Sensing. **42**:679-684.

- Saaty, T.L. (1977). A Scaling Method for Priorities in Hierarchical Structures. *J. Math. Psychology.* **15**:234-241.
- Salman, A. (2000). Using the State-of-the-art Remote Sensing and GIS for monitoring water logging and Salinity, International Water-Management Institute, Lahore, Pakistan.
- Steven, F.G, Zagafos, C. and Oglethorpe, D. (1992). Multi-Criteria Analysis In Soil Salinity: Using Goal Programming To Explore Solutions. *Current Issues in Soil Conservation.* Retrieved on 13.3.2009 from <http://www.multilingualmatters.net/cit/007/0020/cit05200350.pdf>
- Szabolcs, I. (1987). Salt affected soils. Photographic and Videographic observations for determining and mapping the response of cotton to soil salinity, *Remote Sensing of Environment*, CRC Press, Boca Raton, FL, **49**:212-213.
- Tamiru Alemayehu (2003). Controls on the occurrence of cold and thermal springs in central Ethiopia. *African Geoscience Review journal.* **9**:245-248.
- Tamiru Alemayehu (2006). Groundwater occurrence in Ethiopia. Addis Ababa University. Addis Ababa. pp. 82-86.
- Vincent, B., Vidal, A., Tabbet, A.B. and Kuper, M. (1996). Use of satellite remote sensing for the assessment of water logging or salinity. In *Evaluation of performance of subsurface drainage systems: 16th congress on Irrigation and Drainage*, Cairo, Egypt, 15-22 September 1996, ed. B. Vincent, 203-216. New Delhi: International Commission on Irrigation and drainage.
- Voogd, H. (1983). Multi-criteria Evaluation for Urban and Regional Planning. Pion, Ltd., London.
- WWDSE (2001). The study of lake Beseka level (Volume II main report). Water Works Design and Supervision Enterprise (Unpublished report). Ministry of Water Resources, Addis Ababa.

## Appendix-I

Chemical properties of soils of Metehara Sugarcane Estate Irrigation Farm Auger sampled in 2005.

<b>GPS E</b>	<b>GPS N</b>	<b>Auger No.</b>	<b>ECe 1:5,ds/m</b>	<b>pH 1:5</b>
0595402	0982537	<b>2</b>	1.2	<b>8.3</b>
0595725	0972889	<b>3</b>	7.2	<b>8.6</b>
0595773	0969310	<b>5</b>	4.7	<b>8.5</b>
0595808	0973309	<b>7</b>	11.2	<b>8.9</b>
0595933	0972964	<b>9</b>	2.1	<b>8.5</b>
0606394	0976490	<b>10</b>	1.2	<b>8.6</b>
0606553	0976645	<b>12</b>	2.7	<b>8.8</b>
0606479	0976886	<b>14</b>	2.0	<b>8.7</b>
0594288	0975233	<b>18</b>	1.2	<b>8.6</b>
0594379	0975240	<b>23</b>	1.0	<b>8.4</b>
0594389	0975026	<b>25</b>	0.8	<b>8.4</b>
0594299	098025	<b>26</b>	1.1	<b>8.2</b>
0594399	0974825	<b>28</b>	6.3	<b>8.6</b>
0595795	0972308	<b>30</b>	1.3	<b>8.6</b>
0595832	0972068	<b>32</b>	1.3	<b>8.3</b>
0595535	0972289	<b>34</b>	4.5	<b>8.8</b>
0595402	0972537	<b>36</b>	5.6	<b>8.3</b>
0595725	0972889	<b>38</b>	5.3	<b>8.4</b>
0595773	0980100	<b>39</b>	4.7	<b>8.6</b>
0595808	0973309	<b>42</b>	1.1	<b>8.2</b>
0595933	0972964	<b>44</b>	1.0	<b>8.6</b>
0606394	0976490	<b>48</b>	3.1	<b>8.3</b>
0606553	0976645	<b>50</b>	1.2	<b>8.5</b>
0606479	0976886	<b>52</b>	1.0	<b>8.6</b>
0594288	0975233	<b>55</b>	1.2	<b>8.5</b>
0594379	0975240	<b>57</b>	0.9	<b>8.5</b>
0594389	0975026	<b>58</b>	3.1	<b>8.6</b>
0594299	0975025	<b>59</b>	1.1	<b>8.8</b>
0594399	0984825	<b>60</b>	1.4	<b>8.4</b>
0595795	0972308	<b>62</b>	1.0	<b>8.4</b>
0595832	0982068	<b>65</b>	0.9	<b>8.3</b>
0595535	0982289	<b>67</b>	10.2	<b>8.2</b>

<b>GPS E</b>	<b>GPS N</b>	<b>Auger No.</b>	<b>ECe 1:5,ds/m</b>	<b>pH 1:5</b>
0595402	0982537	<b>69</b>	1.0	<b>9.0</b>
0595725	0982889	<b>70</b>	0.8	<b>8.5</b>
0595773	0969310	<b>73</b>	1.2	<b>8.4</b>
0595808	0973309	<b>75</b>	1.1	<b>8.9</b>
0595933	0972964	<b>78</b>	22.5	<b>8.1</b>
0606394	0976490	<b>80</b>	0.9	<b>8.7</b>
0594288	0975233	<b>84</b>	103.1	<b>9.9</b>
0594379	0975240	<b>86</b>	1.1	<b>9.0</b>
0594389	0975026	<b>88</b>	8.5	<b>8.7</b>
0594299	0975025	<b>90</b>	21.9	<b>9.3</b>
0594399	0974825	<b>93</b>	21.2	<b>8.4</b>
0595795	0972308	<b>97</b>	21.1	<b>8.5</b>
0595832	0972068	<b>99</b>	6.8	<b>8.5</b>
0595535	0972289	<b>102</b>	36.5	<b>8.3</b>
0595402	0972537	<b>105</b>	4.6	<b>8.3</b>
0595725	0972889	<b>106</b>	8.8	<b>8.9</b>
0602810	0975870	<b>107</b>	7.7	<b>8.7</b>
0602763	0976068	<b>108</b>	4.1	<b>8.8</b>
0602614	0976232	<b>109</b>	4.7	<b>8.9</b>
0603843	0976909	<b>111</b>	0.8	<b>8.5</b>
0603895	0976705	<b>114</b>	0.5	<b>8.9</b>
0603844	0976506	<b>117</b>	42.0	<b>8.4</b>
0603890	0976300	<b>119</b>	1.3	<b>8.3</b>
0603897	0980281	<b>121</b>	1.8	<b>8.6</b>
0594389	0975026	<b>123</b>	14.1	<b>8.3</b>
0594299	0975025	<b>130</b>	8.2	<b>8.2</b>
0594399	0974825	<b>132</b>	1.4	<b>9.1</b>
0595795	0972308	<b>134</b>	0.8	<b>8.4</b>
0595832	0972068	<b>135</b>	6.0	<b>8.6</b>
0595535	0972289	<b>137</b>	1.3	<b>8.8</b>
0595402	0972537	<b>142</b>	19.8	<b>8.7</b>
0595725	0972889	<b>143</b>	3.5	<b>8.8</b>

<b>GPS E</b>	<b>GPS N</b>	<b>Auger No.</b>	<b>ECe 1:5,ds/m</b>	<b>pH 1:5</b>
0594379	0975240	<b>207</b>	2.0	<b>8.7</b>
0594389	0975026	<b>209</b>	1.5	<b>8.5</b>
0594299	0975025	<b>210</b>	1.4	<b>8.2</b>
0594399	0974825	<b>211</b>	2.3	<b>9.0</b>
0595795	0972308	<b>213</b>	0.4	<b>8.4</b>
0595832	0972068	<b>219</b>	0.8	<b>8.3</b>
0595535	0972289	<b>221</b>	1.5	<b>8.3</b>
0595402	0972537	<b>224</b>	1.5	<b>8.2</b>
0595725	0972889	<b>227</b>	0.6	<b>8.4</b>
0595773	0973100	<b>229</b>	1.3	<b>7.9</b>
0595808	0973309	<b>231</b>	1.6	<b>7.7</b>
0595933	0972964	<b>234</b>	0.7	<b>8.4</b>
0606394	0969490	<b>236</b>	2.7	<b>8.0</b>
0606553	0976645	<b>237</b>	1.1	<b>8.6</b>
0606479	0976886	<b>240</b>	1.0	<b>8.6</b>
0594288	0975233	<b>244</b>	1.4	<b>8.6</b>
0594379	0975240	<b>245</b>	4.1	<b>9.4</b>
0594389	0975026	<b>246</b>	1.3	<b>8.5</b>
0594299	0975025	<b>247</b>	1.2	<b>8.2</b>
0594399	0974825	<b>250</b>	24.3	<b>9.2</b>
0595795	0972308	<b>251</b>	1.0	<b>8.7</b>
0595832	0972068	<b>252</b>	1.5	<b>8.8</b>
0595535	0972289	<b>254</b>	36.5	<b>8.4</b>
0595402	0972537	<b>257</b>	11.0	<b>8.9</b>
0595725	0972889	<b>259</b>	12.1	<b>8.3</b>
0595773	0973100	<b>261</b>	1.2	<b>8.7</b>
0595808	0973309	<b>264</b>	1.0	<b>8.8</b>
0595933	0972964	<b>266</b>	1.4	<b>8.2</b>
0606394	0976490	<b>271</b>	1.1	<b>8.5</b>
0606553	0976645	<b>272</b>	6.2	<b>10.4</b>
0606479	0976886	<b>274</b>	0.9	<b>8.4</b>
0594288	0975233	<b>276</b>	1.0	<b>8.9</b>
0594379	0975240	<b>278</b>	76.7	<b>8.5</b>
0594389	0975026	<b>281</b>	0.8	<b>8.2</b>
0594299	098025	<b>284</b>	1.1	<b>8.3</b>
0594399	0974825	<b>287</b>	8.6	<b>8.4</b>
0595795	0972308	<b>289</b>	1.0	<b>8.7</b>
0595832	0972068	<b>290</b>	1.2	<b>8.5</b>
0595535	0972289	<b>292</b>	2.6	<b>8.4</b>
0595402	0972537	<b>296</b>	11.6	<b>8.7</b>
0595725	0972889	<b>297</b>	1.7	<b>8.6</b>
0595773	0973100	<b>298</b>	0.2	<b>8.3</b>
0595808	0973309	<b>301</b>	1.0	<b>8.3</b>

0595933	0972964	<b>303</b>	1.5	<b>7.6</b>
0606394	0966490	<b>305</b>	0.8	<b>8.7</b>
0606553	0976645	<b>307</b>	1.0	<b>8.1</b>
0606479	0976886	<b>308</b>	10.5	<b>9.3</b>
0594288	0975233	<b>310</b>	1.2	<b>8.1</b>

Source: **General Integrated Rural Development Consultant (GIRDC) (2005, unpublished).**

## Appendix-II

The Ground water table of Metehara Sugarcane Estate Irrigation Farm taken in May 2005.

UTME	UTMN	Elev.m	GWD, m
601066	979955	953.14	2.60
603993	980226	949.50	3.00
592494	986295	981.29	11.94
602168	979920	950.24	1.50
601365	977360	960.00	6.40
600928	977034	960.00	0.76
600874	977318	950.00	12.65
602421	979227	950.00	0.45
599398	976335	960.00	1.32
601176	972623	990.00	8.70
605258	982894	949.80	6.15
594965	969570	987.96	10.43
595410	970871	975.74	2.65
596608	973562	965.23	0.35
602009	979970	950.95	2.80
588625	988621	1004.98	5.80
584990	982082	1101.00	7.50
591516	993908	994.60	3.47
586934	976801	1010.00	6.70
604644	987020	958.10	7.71
604721	979005	959.00	10.18
592530	984297	956.50	2.23
600250	984000	950.00	13.60
600539	980267	953.39	4.04
595426	984300	952.60	1.75
601116	979750	953.36	5.14
600517	982590	953.00	3.71
600305	982301	953.21	3.70
598914	980723	953.02	3.24
593012	982578	953.24	2.30
593035	982691	958.32	8.18
600252	984352	958.93	8.62
596878	976755	955.14	1.20
593389	974555	955.53	2.54
597969	977868	965.16	14.25
600333	977844	953.67	0.62
599118	977968	958.64	0.08
590513	970001	1020.00	18.12
600331	981811	953.42	1.65
600989	982516	952.84	2.85

Source: Metehara Sugar Factory.

## Appendix-III

Accuracy assessments of land-use land-cover map that shown in Figure 4.1.

Land-use land-cover class	Ground truth in %					
	Water logging	Vegetated	Well vegetated	Fallow land	Moderately to slight salt affected	Severely salt affected soil
<b>water logging</b>	<b>88.84</b>	0.6	1.2	1.3	1.98	1.04
<b>Vegetated</b>	5.27	<b>95.8</b>	2.54	0	2.64	0
<b>Well vegetated</b>	0.97	1.5	<b>92.72</b>	0	0.08	0
<b>Fallow land</b>	3.6	0.9	0	<b>94.5</b>	2.07	0.94
<b>Moderately to slight salt affected</b>	1.32	0.8	3.54	1.84	<b>91</b>	2.02
<b>Severely salt affected soil</b>	0	0.4	0	2.36	2.23	<b>96</b>
<b>Total</b>	100	100	100	100	100	100

Overall Accuracy =  $(18974/20371) = 93.14\%$

Kappa Coefficient = 0.8966

## DECLARATION

I hereby declare that the thesis entitled “**Analysis and Mapping of Soil Salinity levels in Metehara Sugarcane Estate Irrigation Farm using Different Models**” has been carried out by me under the supervision of Dr. K. V. Suryabhagavan, Department of Earth Sciences, Addis Ababa University, Addis Ababa during the year 2009 as a part of Master of Science program in Remote Sensing and GIS. I further declare that this work has not been submitted to any other University or Institution for the award of any degree or diploma.

**Afework Mekeberiaw Worku**

Signature: \_\_\_\_\_

Place: Addis Ababa

Date: July, 2009

## CERTIFICATE

This is certified that the dissertation entitled “**Analysis and Mapping of Soil Salinity levels in Metehara Sugarcane Estate Irrigation Farm using Different Models**” is a bonafied work carried out by Afework Mekeberiaaw under my guidance and supervision. This is the actual work done by Afework Mekeberiaaw for the partial fulfillment of the award of the Degree of Master of Science in Remote Sensing and GIS from Addis Ababa University, Addis Ababa, Ethiopia.

**Dr. K. V. Suryabhagavan**

*Lecturer*

*Department of Earth Sciences*

Addis Ababa University

Addis Ababa